ISSN 1023-9855

胸腔醫學

Thoracic Medicine

The Official Journal of Taiwan Society of Pulmonary and Critical Care Medicine

Vol.34 No.2 April 2019

第三十四卷 第二期

中華民國一〇八年四月

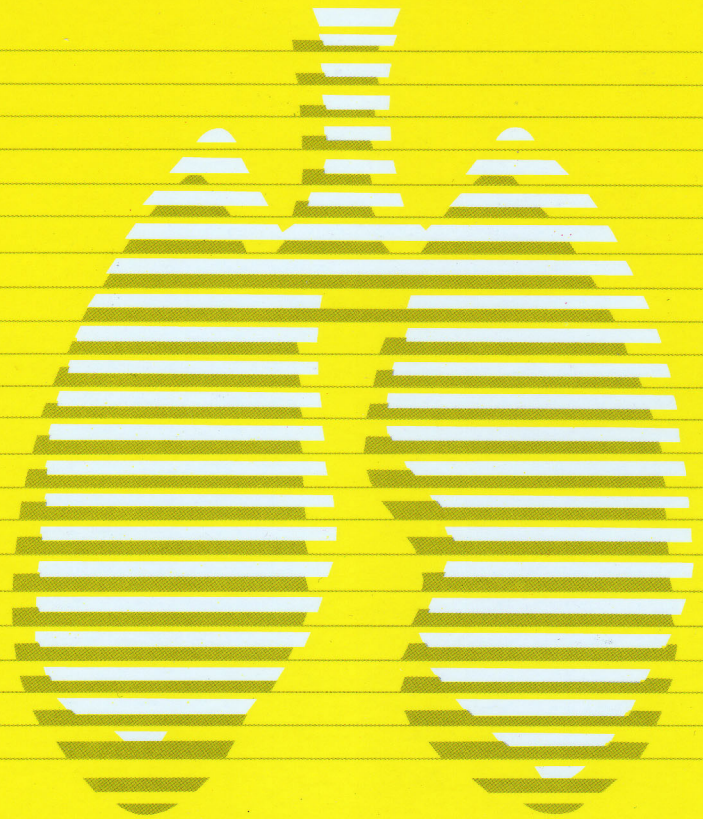

台灣胸腔暨重症加護醫學會

83301 高雄市鳥松區大埤路 123 號

No. 123, Dapi Rd., Niaosong Dist.,
Kaohsiung City 83301, Taiwan

ISSN 1023-9855

中華民國一〇八年四月　第三十四卷　第二期

ISSN 1023－9855

胸腔醫學

Thoracic Medicine

The Official Journal of Taiwan Society of Pulmonary and Critical Care Medicine

Vol.34 No.2 April 2019

原著

病例報告

中華民國一〇八年四月　第三十四卷　第二期

ISSN 1023－9855

Vol.34 No.2 April 2019

胸腔醫學

Thoracic Medicine

The Official Journal of Taiwan Society of Pulmonary and Critical Care Medicine

Orginial Articles

Case Reports

Pectus Excavatum is Associated with a Higher Incidence of Primary Spontaneous Pneumothorax in a Young Population in Taiwan: A Nationwide Population-based Study

Hsu-Kai Huang, Wu-Chien Chien*, Chi-Hsiang Chung**, Ying-Yi Chen, Shih-Chun Lee, Tsai-Wang Huang

Objectives: To investigate the risk of primary spontaneous pneumothorax among patients with pectus excavatum and to evaluate whether they have a higher risk of primary spontaneous pneumothorax than the general population.

Methods: Patient data from the Taiwan National Health Insurance Research Database from January 1, 2000 to December 31, 2013 were collected. A total of 1,652 patients with pectus excavatum and a retrospective matched comparison control cohort of 6,608 individuals were analyzed. Cox regression analyses were performed to determine the risk of primary spontaneous pneumothorax.

Results: The cumulative incidence rate of primary spontaneous pneumothorax was 0.36% in the study group and 0.15% in the control group. Cox regression analysis with adjustment for gender, age, income, urbanization level, and geographic region revealed that pectus excavatum patients were at significantly greater risk of developing primary spontaneous pneumothorax.

Conclusion: Patients with pectus excavatum have a higher risk of developing primary spontaneous pneumothorax. Surgeons should be aware of the risk of bilateral pneumothorax and carefully evaluate these patients before performing corrective surgery using the Nuss procedure. ***(Thorac Med 2019; 34: 47-57)***

Key words: pectus excavatum, spontaneous pneumothorax, funnel chest

Introduction

Pectus excavatum (PE), also known as "funnel chest", is the most common congenital chest wall deformity and manifests as a depression of the middle or lower sternum and associated costal cartilages. The incidence of PE is reported to be approximately 1:400 live births,

Division of Thoracic Surgery, Tri-Service General Hospital, National Defense Medical Center, Taipei, Taiwan; *Department of Medical Research, Tri-Service General Hospital, National Defense Medical Center, Taipei, Taiwan; **School of Public Health, National Defense Medical Center, Taipei, Taiwan

Address reprint requests to: Dr. Tsai-Wang Huang, Division of Thoracic Surgery, Tri-Service General Hospital, National Defense Medical Center, Taipei, Taiwan, No. 325, Section 2, Cheng-Kung Road, Neihu District, Taipei 11490, Taiwan

and males are affected 3 times as often as females [1]. Surgical intervention is usually indicated for patients with cardiopulmonary distress or a Haller index >3.2. The minimally invasive Nuss technique has provided good outcomes in the past 2 decades [2-3].

Primary spontaneous pneumothorax (PSP) is usually caused by a rupture of apical subpleural blebs and air leakage into the pleural cavity. It is more prevalent in tall, thin, and young male populations [4]. Treatment of pneumothorax varies, and includes radiograph follow-up, drainage or surgery. The goal of surgical intervention is to prevent recurrence and life-threatening conditions such as tension pneumothorax. Resection of subpleural blebs and pleurodesis are often applied, but video-assisted thoracoscopic surgery (VATS) is the most common operation performed because it is minimally invasive [5]. In our daily thoracic surgery practice, we may observe a funnel chest and a high Haller index in some PSP patients. However, no studies in the literature have discussed the possible relationship between these 2 diseases. The purpose of this nationwide population-based cohort study was to investigate the association between PE and PSP.

Materials and Methods

Data sources

Taiwan's National Health Insurance Research Database (NHIRD) has been active since the establishment of Taiwan's health care system in 1995. This database includes the medical records of the entire population of approximately 23 million, and National Health Insurance (NHI) coverage was 99.6% in 2009. In our study, data were collected from the Longitudinal Health Insurance Database (LHID), which is a subset database of Taiwan's NHIRD that is released to the public for research purposes. The disease diagnosis codes are based on the International Classification of Diseases, 9th revision, Clinical Modification (ICD-9-CM) diagnosis and procedure codes. The Institutional Review Board of Tri-Service General Hospital approved this study and waived the requirement for written informed consent (TSGHIRB No. 2-105-05-082).

Study design and sampled participants

This was a retrospective cohort design study. Patients with newly diagnosed PE, using ICD-9 code 754.81 (Pectus excavatum), from January 1, 2000 to December 31, 2013, were selected. For the non-PE control cohort, we randomly selected patients without a past history of PE from insured cases. The PE cohort and non-PE control cohort were frequency-matched by age and gender. We chose patients aged between 16 and 40 years because spontaneous pneumothorax seldom occurs after 40 years of age, and the NHI claim code 67045B (Correction of adult chest wall deformity) is used for patients older than 16 years.

Outcome measures

All study participants were followed from the index date. PSP cases with ICD-9-CM code 512.0 (Spontaneous tension pneumothorax), 512 (Pneumothorax and air leak) or 512.81 (Primary spontaneous pneumothorax) were included. The exclusion codes were 512.82 (Secondary spontaneous pneumothorax), 860 (Traumatic pneumothorax), 011.71 (Tuberculous pneumothorax), and 759.82 (Marfan syndrome). The patients' data were reviewed for NHI claim codes 67045B (Correction of adult chest wall deformity), 67048B (Thoracoscopic

pleurodesis), 67051B (Thoracoscopic wedge or partial resection of the lung), 56010B (Chest intubation) and 67006B (Closed drainage).

Variates included gender, age group (16-29, 30-39 years), geographical area of residence (north, center, south and east of Taiwan), urbanization level of residence (level 1 to 4), and monthly income (in New Taiwan Dollars [NTD]; <18,000, 18,000-34,999, and ≥35,000).

Statistical analysis

All analyses were performed using SPSS software version 22 (SPSS Inc., Chicago, Illinois, USA). The χ^2 and *t*-tests were used to evaluate differences between the groups with and without PE at baseline and at the study endpoint. The difference in the risk of PSP between the study and control groups was estimated using the Kaplan-Meier method, with the log-rank test to assess the occurrence of cumulative risk, and the results are presented as hazard ratios (HRs) with 95% confidence intervals (CIs). A 2-tailed *p*-value <0.05 was considered to indicate statistical significance.

Results

A total of 3,946 patients with PE were identified in the NHIRD, which contains data on 1,978,496 individuals. All patients were between 16 and 40 years of age. After exclusion based on the above exclusion criteria and matching according to gender, age group and index year, there were 1,652 cases in the PE group, and 6,608 controls in the propensity score-matched non-PE group (Figure 1). The characteristic features of both groups at baseline and at the end of the study are listed in Tables 1 and 2. There were no significant differences in gender, age or insured premium. Compared with the controls, the PE group had a lower Charlson Comorbidity Index (CCI) (0.02 vs. 0.14, $p<0.001$) and more frequently lived in urbanized areas of northern Taiwan ($p<0.001$). The PE group tended to be diagnosed in the summer (44.6% vs 26.41%; $p<0.001$). The proportions of those living in northern Taiwan, in a higher urbanized area and with a better hospital level of care were higher in the PE group than in the non-PE group.

The cumulative incidence of PSP was 0.36% (6/1652) and 0.15% (10/6608), respectively, in the PE and non-PE groups. Using the Kaplan-Meier method, the cumulative risk of developing PSP differed significantly between the PE and non-PE groups ($p<0.001$) (Figure 2). Cox regression and controlling factors such as gender, age, season, urbanization level, and insured premium revealed that the PE group had a HR of 7.83 ($p=0.002$) of experiencing PSP, compared with the non-PE group. Using stratified variables, the PE 16-29-year-old age group had a HR of 7.969 of developing PSP compared to the non-PE group (Tables 3 and 4). Other factors showed no significant difference.

Discussion

In this population-based study, we observed that patients with PE had a 7.83-fold increased risk of developing PSP, and there was a positive correlation between PE and PSP. We assumed that PE is associated with a higher incidence of developing PSP. The case of a 17-year-old male who developed bilateral pneumothorax after undergoing the Nuss procedure was recently reported from Japan. The cause of the pneumothorax was found to be a bulla at the left apex of the lung with spontaneous rupture, and air went into the right pleural cavity through

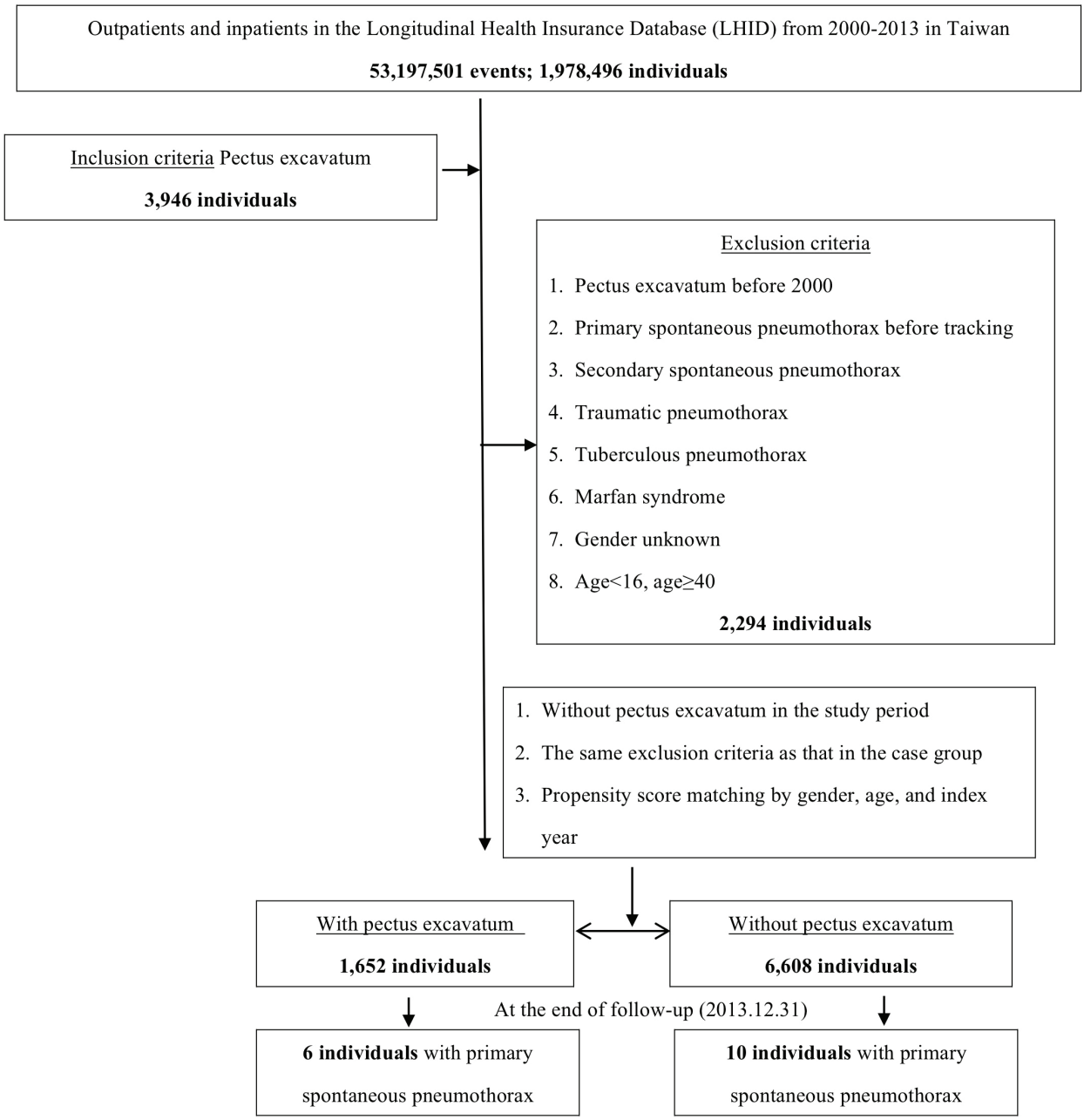

Fig. 1. Flowchart of study sample selection from the National Health Insurance Research Database in Taiwan
Pectus excavatum: ICD-9-CM 754.81; Primary spontaneous pneumothorax: ICD-9-CM 512.0, 512.8; Secondary spontaneous pneumothorax: ICD-9-CM 512.82; Traumatic pneumothorax: ICD-9-CM 860; Tuberculous pneumothorax: ICD-9-CM 011.71; Marfan syndrome: ICD-9-CM 759.82

the substernal tunnel created for the Nuss bar. Video-assisted thoracoscopic wedge resection was then performed without recurrence [6]. Although the exact mechanism regarding the relationship between PE and PSP is still unclear, some hypotheses have been proposed. Previous

Table 1. Baseline Patient Characteristics

Baseline patient characteristics							
Pectus excavatum	Total		With		Without		*P*
Variables	n	%	n	%	n	%	
Total	8,260		1,652	20.00	6,608	80.00	
Gender							0.999
Male	6,455	78.15	1,291	78.15	5,164	78.15	
Female	1805	21.85	361	21.85	1,444	21.85	
Age (years)	24.76±5.54		23.43±5.39		25.10±5.52		0.248
Age group (years)							0.999
16-29	7,090	85.84	1,418	85.84	5,672	85.84	
30-39	1,170	14.16	234	14.16	936	14.16	
Charlson Comorbidity Index (CCI)	0.11±0.68		0.02±0.20		0.14±0.75		<0.001
Season							<0.001
Spring	1,965	23.79	247	14.95	1,718	26.00	
Summer	2,483	30.06	739	44.73	1,744	26.39	
Autumn (September-November)	1,852	22.42	317	19.19	1,535	23.23	
Winter (December-February)	1,960	23.73	349	21.13	1,611	24.38	
Location							<0.001
Northern Taiwan	3,710	44.92	1,159	70.16	2,551	38.60	
Central Taiwan	2,304	27.89	242	14.65	2,062	31.20	
Southern Taiwan	1,848	22.37	223	13.50	1,625	24.59	
Eastern Taiwan + Outlying islands	398	4.82	28	1.69	370	5.60	
Urbanization level							<0.001
1	2,684	32.49	543	32.87	2,141	32.40	
2	3,488	42.23	858	51.94	2,630	39.80	
3	861	10.42	107	6.48	754	11.41	
4 (The lowest)	1,227	14.85	144	8.72	1,083	16.39	
Level of care							<0.001
Medical hospital	1,542	36.20	570	66.90	972	28.52	
Regional hospital	1,301	30.54	184	21.60	1,117	32.78	
Local hospital	1,417	33.26	98	11.50	1,319	38.70	
Insured premium (NT$)							0.302
<18,000	4,161	97.68	838	98.36	3,323	97.51	
18,000-34,999	56	1.31	7	0.82	49	1.44	
≥35,000	43	1.01	7	0.82	36	1.06	

P-value (categorical variables: Chi-square/Fisher's exact test; continuous variables: *t*-test)

Table 2. Patient Characteristics at the End of Follow-up

Patient characteristics at the end of follow-up							
Pectus excavatum	Total		With		Without		*P*
Variables	n	%	n	%	n	%	
Total	4,260		852	20.00	3,408	80.00	
Primary spontaneous pneumothorax							0.043
Without	4,252	99.81	849	99.65	3,403	99.85	
With	8	0.19	3	0.35	5	0.15	
Gender							0.999
Male	3,330	78.17	666	78.17	2,664	78.17	
Female	930	21.83	186	21.83	744	21.83	
Age (years)	27.20±6.61		24.01±5.39		27.99±6.65		0.053
Age group (years)							0.120
16-29	3,457	81.15	722	84.74	2,735	80.25	
30-39	803	18.85	130	15.26	673	19.75	
Charlson Comorbidity Index (CCI)	0.20±1.10		0.04±0.29		0.24±1.21		<0.001
Season							**<0.001**
Spring	940	22.07	121	14.20	819	24.03	
Summer	1,263	29.65	335	39.32	928	27.23	
Autumn (September-November)	1,057	24.81	201	23.59	856	25.12	
Winter (December-February)	1,000	23.47	195	22.89	805	23.62	
Location							<0.001
Northern Taiwan	1,942	45.59	591	69.37	1,351	39.64	
Central Taiwan	1,153	27.07	126	14.79	1,027	30.13	
Southern Taiwan	956	22.44	119	13.97	837	24.56	
Eastern Taiwan + Outlying islands	209	4.91	16	1.88	193	5.66	
Urbanization level							<0.001
1	1,374	32.25	288	33.80	1,086	31.87	
2	1,851	43.45	438	51.41	1,413	41.46	
3	435	10.21	46	5.40	389	11.41	
4 (The lowest)	600	14.08	80	9.39	520	15.26	
Insured premium (NT$)							0.120
<18,000	8,066	97.65	1,624	98.31	6,442	97.49	
18,000-34,999	109	1.32	14	0.85	95	1.44	
≥35,000	85	1.03	14	0.85	71	1.07	

P-value (categorical variables: Chi-square/Fisher's exact test; continuous variables: *t*-test)

data showed that patients with a lower BMI tended to develop PSP [7]. An associated hypothesis is that taller individuals have a higher distending pressure on the alveoli at the apex of the lung. This higher pressure could be related to the trapping of subpleural air and bleb forma-

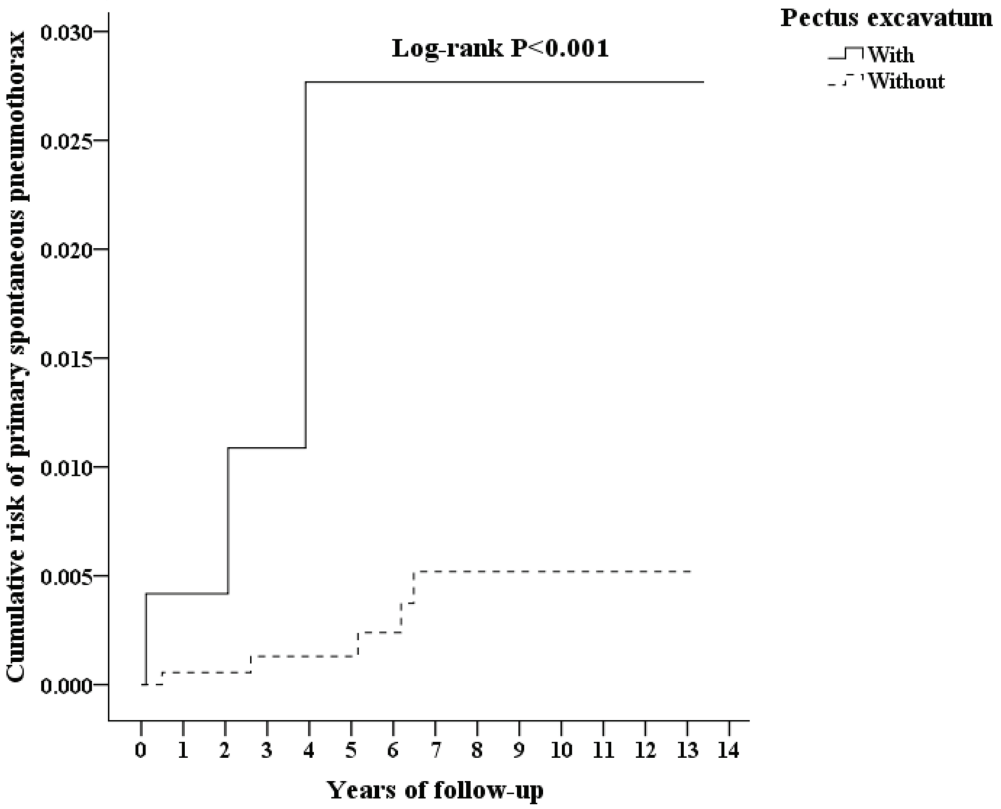

Fig. 2. Kaplan-Meier curve for the cumulative risk of primary spontaneous pneumothorax among patients aged 16-39 years stratified by pectus excavatum using a log-rank test

tion [7]. Casha *et al*. reported a biomechanical hypothesis regarding apical lung disease [8]. They used chest radiographs and computerized tomography images to investigate rib cage measurements in male pneumothorax patients and control groups. To assess pleural stress, a finite element analysis model was developed, which revealed a 20-fold increase in pleural stress in the apex of the chest, with a low thoracic index typical of spontaneous pneumothorax patients, and stress that was magnified by coughing in an antero-posteriorly flattened chest in individuals with a low BMI [9]. Park *et al*. performed a cross-sectional study on growth in PE patients [10]. Data on body measurements of height, weight, BMI and the Haller index were collected, and the findings showed that growth in PE patients is slowed compared with that in the normal population. After corrective surgery, weight and BMI remained low, but height was restored. Therefore, correction of the deformity may have some positive effects on growth.

We have some theories on the seasonal and geographic differences between the 2 groups in Tables 1 and 2, based on our thoracic surgery practice. Patients with PE often have a higher socioeconomic status and usually seek medical advice or surgical intervention during summer vacation. The above observation is compatible with our results.

Our study showed that young PE patients had a 7.83-fold increased risk of developing

Table 3. Primary Spontaneous Pneumothorax Factors at the End of Follow-up Using Cox Regression

Primary spontaneous pneumothorax factors at the end of follow-up using Cox regression								
Variables	Crude HR	95% CI	95% CI	*P*	Adjusted HR	95% CI	95% CI	*P*
Pectus excavatum								
Without	Reference				Reference			
With	12.313	3.955	38.336	<0.001	7.830	2.114	29.004	0.002
Gender								
Male	1.977	0.449	8.702	0.367	1.534	0.339	6.932	0.578
Female	Reference				Reference			
Age (years)	0.758	0.674	0.855	<0.001				
Age group (years)								
16-29	Reference				Reference			
30-39	0.373	0.132	1.050	0.062	0.552	0.232	3.023	0.328
Charlson Comorbidity Index (CCI)	1.211	1.055	1.391	0.006	1.265	0.303	3.871	0.007
Season								
Spring	Reference				Reference			
Summer	1.129	0.319	4.004	0.851	0.837	0.232	3.023	0.786
Autumn (September-November)	1.135	0.320	4.024	0.844	1.083	0.303	3.871	0.903
Winter (December-February)	0.000	-	-	0.958	0.000	-	-	0.961
Location					Had multicollinearity with urbanization level			
Northern Taiwan	Reference				Had multicollinearity with urbanization level			
Middle Taiwan	0.000	-	-	0.970	Had multicollinearity with urbanization level			
Southern Taiwan	0.224	0.051	0.986	0.048	Had multicollinearity with urbanization level			
Eastern Taiwan + Outlying islands	0.000	-	-	0.979	Had multicollinearity with urbanization level			
Urbanization level								
1	Reference				Reference			
2	0.710	0.267	1.893	0.494	0.900	0.325	2.490	0.839
3	0.000	-	-	0.981	0.000	-	-	0.981
4 (The lowest)	0.000	-	-	0.976	0.000	-	-	0.975
Insured premium (NT$)								
<18,000	Reference				Reference			
18,000-34,999	0.000	-	-	0.760	0.000	-	-	0.991
≥35,000	0.000	-	-	0.813	0.000	-	-	0.995

HR: hazard ratio, CI: confidence interval, Adjusted HR: Adjusted variables listed in the table

PSP. The possible reason may be that PE tends to lead to retarded growth and low BMI, which is correlated with higher pleural stress in the lung apex, which then causes blebs or bulla formation.

There are some limitations to our study. This was a retrospective study, and the NHIRD does not contain detailed information on pa-

Table 4. Primary Spontaneous Pneumothorax Factors at the End of Follow-up Stratified by Variables Listed in the Table Using Cox Regression

Primary spontaneous pneumothorax factors at the end of follow-up stratified by variables listed in the table using Cox regression											
Pectus excavatum	With			Without			Ratio	Adjusted	95%CI	95%CI	*P*
Variables	Event	PYs	Rate (per 105 PYs)	Event	PYs	Rate (per 105 PYs)		HR			
Total	6	9,930.45	60.42	10	40,223.10	24.86	2.430	7.830	2.114	29.004	0.002
Gender											
Male	4	8,381.56	47.72	10	31,142.65	32.11	1.486	5.097	1.212	21.439	0.026
Female	2	1,548.89	129.12	0	9,080.45	0.00	-	-	-	-	-
Age group (years)											
16-29	6	8,354.97	71.81	4	14,533.74	27.52	2.609	7.969	1.578	40.240	0.012
30-39	0	1,575.48	0.00	6	25,689.36	23.36	0.000	0.000	-	-	0.990
Season											
Spring	0	1,714.54	0.00	4	8,598.21	46.52	0.000	0.000	-	-	0.996
Summer	4	3,286.00	121.73	2	11,136.82	17.96	6.778	3.851	0.638	23.248	0.142
Autumn (September-November)	2	2,565.71	77.95	4	11,549.04	34.63	2.251	7.567	0.764	74.947	0.084
Winter (December-February)	0	2,364.20	0.00	0	8,939.03	0.00	-	-	-	-	-
Urbanization level											
1	4	4,029.44	99.27	4	11,661.39	34.30	2.894	9.112	0.015	70.419	0.359
2	2	4,998.31	40.01	6	16,694.21	35.94	1.113	2.420	0.304	19.289	0.404
3	0	258.93	0.00	0	4,656.67	0.00	-	-	-	-	-
4 (The lowest)	0	643.77	0.00	0	7,210.83	0.00	-	-	-	-	-
Insured premium (NT$)											
<18,000	6	9,679.47	61.99	10	39,371.13	25.40	2.440	7.830	2.114	29.004	0.002
18,000-34,999	0	117.59	0.00	0	531.42	0.00	-	-	-	-	-
≥35,000	0	73.39	0.00	0	320.55	0.00	-	-	-	-	-

PYs: Person-years; Adjusted HR: Adjusted hazard ratio: Adjusted for the variables listed in the Cox regression table; CI: confidence interval

tients' weight, height, BMI or Haller index. Furthermore, patients with PE without symptoms or a lower Haller index may not be registered in this database. This may be related to the relatively small patient population. We also could not assess the imaging studies to verify lung conditions, including bleb formation. Further studies are required to clarify the relationship between PE and PSP.

We suggest that in the evaluation of a PE patient with a low BMI and a high Haller index based on a CT scan, bleb formation should be assessed at the apex. Surgeons should consider surgical intervention with correction of the deformity and bleb resection at the same time, due to the higher risk of PSP development and greater operative difficulty because of subsequent pleural adhesions or possible life-threat-

ening bilateral pneumothorax after the Nuss procedure.

References

1. Hebra A. Minimally invasive repair of pectus excavatum. Semin Thorac Cardiovasc Surg 2009 Spring; 21(1): 76-84.
2. Croitoru DP, Kelly RE, Jr., Goretsky MJ, *et al*. Experience and modification update for the minimally invasive Nuss technique for pectus excavatum repair in 303 patients. J Pediatr Surg 2002 Mar; 37(3): 437-45.
3. Nuss D, Kelly RE, Jr., Croitoru DP, *et al*. A 10-year review of a minimally invasive technique for the correction of pectus excavatum. J Pediatr Surg 1998 Apr; 33(4): 545-52.
4. Baumann MH, Noppen M. Pneumothorax. Respirology 2004; 9(2): 157-64.
5. MacDuff A, Arnold A, Harvey J, Group BTSPDG. Management of spontaneous pneumothorax: British Thoracic Society Pleural Disease Guideline 2010. Thorax 2010 Aug; 65 Suppl 2: ii18-31.
6. Matsuoka S, Miyazawa M, Kashimoto K, *et al*. A case of simultaneous bilateral spontaneous pneumothorax after the Nuss procedure. Gen Thorac Cardiovasc Surg 2016 Jun; 64(6): 347-50.
7. Huang TW, Cheng YL, Tzao C, *et al*. Factors related to primary bilateral spontaneous pneumothorax. Thorac Cardiovasc Surg 2007 Aug; 55(5): 310-2.
8. Casha AR, Manche A, Gatt R, *et al*. Is there a biomechanical cause for spontaneous pneumothorax? Eur J Cardiothorac Surg 2014 Jun; 45(6): 1011-6.
9. Casha AR, Manche A, Camilleri L, *et al*. A biomechanical hypothesis for the pathophysiology of apical lung disease. Med Hypotheses 2016 Jul; 92: 88-93.
10. Park HJ, Kim JJ, Park JK, *et al*. A cross-sectional study for the development of growth of patients with pectus excavatum. Eur J Cardiothorac Surg 2016 Oct; 50(6): 1102-9.

漏斗胸與原發性自發性氣胸具有相關性：台灣健保資料庫研究

黃敍愷　簡戊鑑 *　鍾其祥 **　陳穎毅　李世俊　黃才旺

漏斗胸（ICD-9-CM 754.81）是否較一般族群更容易增加自發性氣胸（ICD-9-CM 512.0 + ICD-9-CM 512.8）的風險。

臨床上偶而有男性瘦高病人因自發性氣胸來診發現有漏斗胸情形，或是因為漏斗胸來診於電腦斷層中發現異常肺泡組織（可能導致原發性自發性氣胸），以百萬歸人檔處理，希望可以看到其意義。

使用百萬歸人檔做回溯性分析，並以一比四做配對，可找出漏斗胸組 1,652 人及一般組 6,608 人，並使用迴歸分析來判斷發生自發性氣胸之風險。

結果：在累積自發性氣胸之發生率，可發現漏斗胸組為 0.36% 大於一般組的 0.15%，經過調整性別，年齡，投保級距及居住地都市化程度後，發現漏斗胸組別有較高風險發生自發性氣胸（Hazard ratio: 7.83, 95% CI 2.114-29.004, p=0.002）。

結論：漏斗胸族群與自發性氣胸之族群有高相關性，由於以納式微創矯正術治療可能導致雙側肋膜腔交通，若發生氣胸可能造成嚴重且致命的雙側氣胸，外科醫師在術前評估時，應考量有無原發性自發性氣胸的危險因素如斷層掃描發現異常肺泡等再行手術。*(胸腔醫學* ***2019; 34: 47-57)***

關鍵詞：漏斗胸，自發性氣胸

國防醫學院三軍總醫院　外科部　胸腔外科，* 國防醫學院三軍總醫院　醫學研究室，** 國防醫學院　公共衛生研究所
索取抽印本請聯絡：黃才旺醫師，國防醫學院三軍總醫院　外科部　胸腔外科，台北市內湖區成功路二段 325 號

Delayed Photosensitivity Dermatitis Caused by Crizotinib

Jeng-Shiuan Tsai*,**, Chao-Kai Hsu***, Hsin-San Yang***, Yu-Lin Ting**, Chien-Chung Lin*,**, Chang-Wen Chen*,**

Crizotinib is used as first-line treatment for anaplastic lymphoma kinase (ALK)-positive advanced lung adenocarcinoma. Commonly reported toxicities include visual disturbance, diarrhea, transaminitis, fatigue, and edema. In phase I and phase III trials of crizotinib, rashes were reported in patients at frequencies of 11% and 9%, respectively. Most of these patients developed a skin rash (photosensitivity dermatitis) just after taking crizotinib or within 1 to 2 months thereafter. The patient reported here developed delayed photosensitivity dermatitis after taking crizotinib for 6 months. The patient's rash was likely caused by crizotinib, since it persisted when other medications were discontinued, but resolved after crizotinib was held. The rash flared up again after re-challenging. The skin rash was characterized by itchy plaques on the 4 extremities, classified as grade II. Skin biopsy was performed and the pathological finding was compatible with drug-related photosensitivity dermatitis. After the dosage of crizotinib was adjusted, the patient's skin rash became less severe, and was tolerable. It is unusual for patients taking crizotinib to develop delayed photosensitivity. The associated etiologies remain uncertain and may be mediated by ALK inhibition itself, an off-target effect, or by host immunity to crizotinib. ***(Thorac Med 2019; 34: 58-63)***

Key words: crizotinib, photosensitivity dermatitis, ALK-positive lung cancer

Introduction

The echinoderm microtubule-associated protein-like 4-anaplastic lymphoma kinase (EML4-ALK) oncogene fusions is seen in approximately 2-7% of patients with lung adenocarcinomas and these patients respond to crizotinib, an oral ATP-competitive selective inhibitor of ALK [1-2]. The phase III trial noted visual disturbances, gastrointestinal symptoms and skin rash as common adverse events but most skin rash developed within one to two months. We present a patient who developed delayed photosensitivity dermatitis six months after beginning crizotinib.

*Division of Chest Medicine, **Department of Internal Medicine, ***Department of Dermatology, National Cheng Kung University Hospital, College of Medicine, National Cheng Kung University, Tainan, Taiwan
Address reprint requests to: Dr. Chien-Chung Lin, Division of Chest Medicine, Department of Internal Medicine, National Cheng Kung University Hospital, College of Medicine, National Cheng Kung University, 138 Sheng-Li Road, Tainan 704, Taiwan

Case Report

An 81-year-old man, a never-smoker, visited our clinic because he had developed a productive cough with yellowish and blood-tinged sputum for 1 month. Chest X-ray taken in July 2015 revealed a right lower lung (RLL) lesion. We arranged for a chest computed tomography (CT) scan with contrast, which revealed a lobular mass in the RLL, about 7.3 cm in maximal diameter, abutting the medial pleura. On August 11, 2015, CT-guided lung biopsy was performed; the biopsy report was consistent with lung mucinous adenocarcinoma. An anaplastic lymphoma kinase (ALK) (2p23) rearrangement was detected using the US Food and Drug Administration (FDA)-approved fluorescence in situ hybridization assay. Brain magnetic resonance imaging and a whole-body bone scan both showed no evidence of metastatic disease. Since the lung cancer was classified as stage IIB, the patient underwent video-assisted thoracoscopic surgery for RLL lobectomy on September 25, 2015. Although adjuvant chemotherapy was suggested, the patient refused and asked to continue observation at our clinic. However, elevated carcinoembryonic antigen was noted and a chest CT scan on July 15, 2016, showed new lesions at the right upper lung and right middle lung. New metastasis lesions were favored, and he began chemotherapy with cisplatin and pemetrexed. Cisplatin was eventually discontinued due to severe nausea and vomiting, and a follow-up chest CT scan taken on November 11, 2016, revealed an interval progression of tumor size (Figure 1A). Crizotinib (Xalkori) 250 mg PO twice daily was prescribed in December. Tumor size decreased after treatment for 9 months, as shown in the follow-up CT scan taken in August 2017 (Figure 1B).

During the treatment course, the patient developed asymptomatic hepatitis, which resolved after silymarin usage. Then, asymptomatic erythematous plaques with scaling on the face and 4 extremities in sun-exposed areas appeared in June, 2017 (Figure 2A). As the rash evolved, there were marked areas of exfoliation. Skin

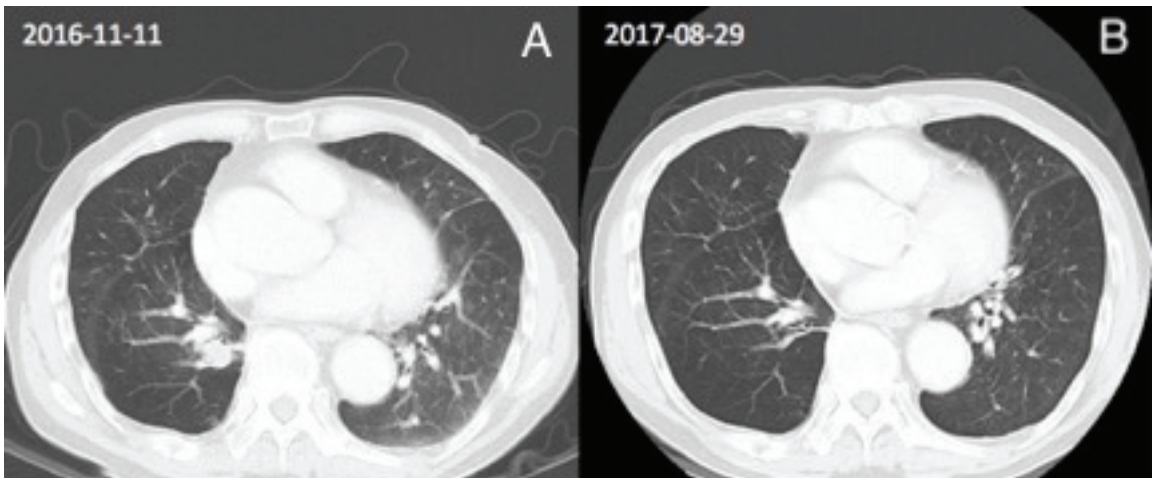

Fig. 1. Chest CT images showing lung cancer response to crizotinib. (A) CT image during the second cycle of chemotherapy with cisplatin plus pemetrexed showing a lung mass at the right middle lobe, and (B), CT image taken after treatment with crizotinib for 9 months showing a decreased lung mass compared with the previous image.

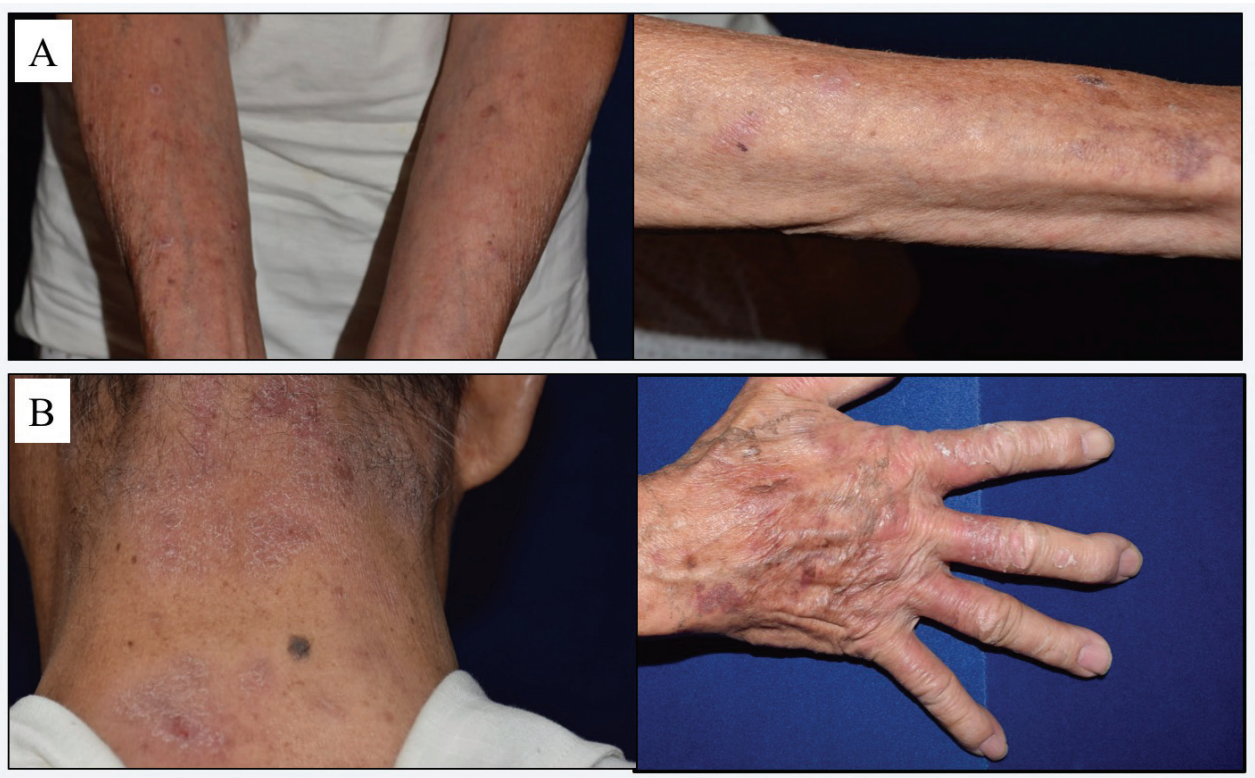

Fig. 2. Photographs of skin photosensitivity dermatitis. Images of exfoliative photosensitive rash after treatment with crizotinib. (A) Representative images showing rash in sun-exposed areas, and close-up view of the right upper extremity showing exfoliation. (B) Newly developed skin rash after crizotinib re-challenge revealing erythematous to violaceous plaques with scaling on the neck and right hand.

biopsy from the right forearm showed vacuolar interface dermatitis, suggesting drug eruption (Figure 3). He was started on prednisolone 5 mg twice per day, levocetirizine, and topical steroid, with crizotinib withheld, on June 26, 2017, and his rash improved 2 weeks later. Then, systemic steroid was held, but levocetirizine and topical steroid were maintained. He was continued on crizotinib with a 50% dose reduction (250 mg PO once daily) on July 14, 2017, and then twice daily on August 4, 2017. However, after re-challenge with a full dose of crizotinib for 1 week (August 11, 2017), his rash flared up again with erythematous to violaceous plaques and scaling on the dorsal hands, face, ears, and upper back (Figure 2B). Throughout this time, all his other medications, including pantoprazole and bumetanide, were maintained, so they were unlikely to have contributed to the development of his photosensitive rash. The skin rash this time was less severe than the first episode, and the patient was able to tolerate it with the usage of levocetrizine and topical steroid (betamethasone), without systemic steroid. He continued using crizotinib for another 6 months. The patient had no other side effects besides the photosensitive rash and 1 episode of hepatitis. After using crizotinib for a total of 15 months, CT scans showed signs of progression; the patient stopped treatment with crizotinib and switched to a second-generation anti-ALK therapy (Alectinib, Roche).

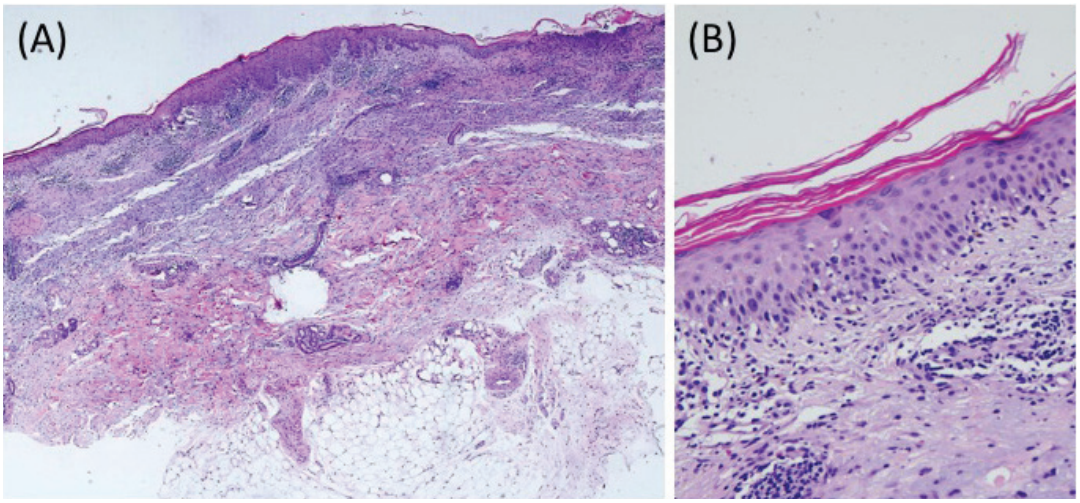

Fig. 3. Photographs of skin biopsy pathology findings. (A) The epidermis shows slight hyperkeratosis with superficial ulceration, and the dermis shows superficial perivascular inflammatory infiltrates. (B) A higher power view illustrates the vacuolar change at the dermoepidermal junction.

Discussion

Here, we reported a patient with ALK-positive metastatic lung adenocarcinoma who developed a photosensitive rash as a reaction to crizotinib. Crizotinib is approved by the US FDA for the treatment of ALK-positive advanced lung adenocarcinoma. Commonly reported toxicities in clinical trials include visual disturbance, diarrhea, transaminitis, fatigue, and edema. In both phase I and phase III trials [1-2], rashes were reported in patients receiving crizotinib at frequencies of 11% and 9%, respectively, with no reported grade III or IV rashes. The rash that our patient developed was likely caused by crizotinib, as he developed the same rash after exposure to crizotinib around 6 months later, and the rash improved after crizotinib was discontinued. The rash was classified as grade II given the marked areas of exfoliation. A case of severe photosensitivity dermatitis caused by crizotinib has been reported [6]. However, to our knowledge, ours is the first report of a delayed photosensitive exfoliative rash due to crizotinib use.

On-target toxicities, such as rash associated with tyrosine kinase inhibitors (TKIs) of the epidermal growth factor receptor (EGFR) signaling pathway or hypertension with monoclonal antibody of the vascular endothelial growth factor receptor signaling pathway, are classic and therefore difficult to prevent by designing different active molecules. Skin toxicity is a common and well-known side effect EGFR inhibitors, such as erlotinib and afatinib, since EGFR is highly expressed in epidermal cells [3]. In contrast, photosensitive dermatitis is not commonly associated with small-molecule TKIs, but has been described in patients taking imatinib [4] and vandetanib [5]. It is unusual for patients taking crizotinib to develop photosensitive dermatitis and also unpredictable. A previous case report described photosensitivity dermatitis caused by crizotinib [6]. The patient reportedly developed a photosensitive rash after taking crizotinib less than 2 months, and the

rash did not completely resolve until 6 weeks after permanently discontinuing crizotinib. Small molecule kinase inhibitors have become the standard treatment and improve the prognosis of many cancer types. But hypersensitivity reactions to these agents interfere with patients receiving these life-prolonging therapies and become a major treatment barrier. Standardized desensitization protocols can overcome this therapeutic barrier by helping patients tolerate drug allergens [7]. Though we did not follow the desensitization protocols, we adjusted the dosage of crizotinib after photosensitivity dermatitis appeared. The patient we reported developed photosensitive exfoliative rashes that were successfully controlled using an antihistamine and a steroid. The patient then could tolerate the side effects and continued to take crizotinib.

Conclusion

Although drug-induced dermatitis is common with TKIs, delayed photosensitivity dermatitis is seldom noted in patients taking ALK inhibitors. The patient in this case report developed photosensitive exfoliative rashes, which were successfully controlled by adjusting the dosage of crizotinib and using an antihistamine and a steroid. Further studies and clinical evidence are needed to determine the associated mechanisms and guidelines for the treatment of skin toxicity related to ALK inhibitors.

References

1. Camidge DR, Bang YJ, Kwak EL, *et al*. Activity and safety of crizotinib in patients with ALK-positive non-small-cell lung cancer: updated results from a phase 1 study. Lancet Oncol 2012; 13: 1011-9.
2. Shaw AT, Kim DW, Nakagawa K, *et al*. Crizotinib versus chemotherapy in advanced ALK-positive lung cancer. N Engl J Med 2013; 368: 2385-94.
3. Mok TS, Wu YL, Thongprasert S, *et al*. Gefitinib or carboplatin-paclitaxel in pulmonary adenocarcinoma. N Engl J Med 2009; 361: 947-57.
4. Brazzelli V, Muzio F, Manna G, *et al*. Photoinduced dermatitis and oral lichenoid reaction in a chronic myeloid leukemia patient treated with imatinib mesylate. Photodermatol Photoimmunol Photomed 2012; 28: 2-5.
5. Kong HH, Fine HA, Stern JB, *et al*. Cutaneous pigmentation after photosensitivity induced by vandetanib therapy. Arch Dermatol 2009; 145: 923-5.
6. Oser MG, Jänne PA. A severe photosensitivity dermatitis caused by crizotinib. J Thorac Oncol 2014; 9, (7): e51-3.
7. Sánchez-López J, Viñolas N, Muñoz-Cano R, *et al*. Successful oral desensitization in a patient with hypersensitivity reaction to crizotinib. J Investig Allergol Clin Immunol 2015; 25(4): 307-8.

截剋瘤引發延遲光敏感性皮膚炎

蔡政軒 *,** 許釗凱 *** 楊省三 *** 丁育麟 ** 林建中 *,** 陳昌文 *,**

截剋瘤（Crizotinib）是目前末期肺癌中為治療間變性淋巴瘤激酶（ALK）陽性的第一線藥物，然而這種藥物最常被提出的副作用包含視覺障礙、腹瀉、轉胺酶增加、疲倦和水腫。在第一期和第三期臨床試驗中，約有 9% 至 11% 的病人會在藥物使用的一到兩個月內出現皮疹（光敏感性皮膚炎）的情況。我們所提供的這個案例是在使用藥物約六個月之後才開始出現皮疹，而皮疹在停用其他藥物之後仍持續存在並且在停用截剋瘤的之後才獲得改善，而當再度使用截剋瘤之後皮疹復發。這些皮疹主要以在四肢出現二級騷癢性丘疹為表現。這些病情變化表示皮疹極可能是截剋瘤所造成。在調低藥物劑量之後，病人皮疹的狀況亦有減輕並且可以忍受的情況。此延遲光敏感性皮膚炎的情況在這類病人之中並不常見，相關的病因機轉目前仍不清楚，或許和藥物本身有關，或許是非目標基因（off target effect）的效果或是宿主免疫系統對截剋瘤所產生的反應。*(胸腔醫學 **2019; 34: 58-63**)*

關鍵詞：截剋瘤 Crizotinib，光敏感性皮膚炎，間變性淋巴瘤激酶陽性肺癌 ALK

成功大學附設醫院 內科部 ** 胸腔內科 *，成功大學附設醫院 皮膚科 ***
索取抽印本請聯絡：林建中醫師，成功大學附設醫院 內科部 胸腔內科，704 台南市北區勝利路 138 號

Pulmonary Melioidosis Associated with Organizing Pneumonia: A Case Report

Ching-Yi Chen*, Yu-Feng Wei*, Chien-Tung Chiu*,**

Melioidosis is a tropical infectious disease caused by *Burkholderia pseudomallei*, which affects the lungs most frequently. Organizing pneumonia (OP) can be cryptogenic or secondary to lung infections, and is rarely associated with melioidosis. We report the case of a 64-year-old male patient who presented with solitary pulmonary opacity that progressed to fulminant septicemia under treatment with empiric antibiotics and oral steroid. The pathology report showed organizing pneumonia, and *B. pseudomallei* was isolated from the blood. The patient recovered very well after treatment was shifted to imipenem/cilastatin plus sulfamethoxazole-trimethoprim. ***(Thorac Med 2019; 34: 64-70)***

Key words: *Burkholderia pseudomallei*, pulmonary melioidosis, organizing pneumonia

Introduction

Melioidosis is a tropical infectious disease of humans and animals caused by *Burkholderia pseudomallei*, which affects the lungs most frequently [1-4]. Organizing pneumonia can be secondary to lung injury or lung pathogens, or cryptogenic with a pathological hallmark, and is rarely associated with melioidosis. [4-5] Solitary pulmonary opacity is a common radiologic finding; it is an unusual presentation of organizing pneumonia and should be differentiated from malignancy. We report the case of a 64-year-old man who presented with solitary pulmonary opacity, which biopsy reported as organizing pneumonia; *B. pseudomallei* was isolated in the pathology study.

Case Report

This 64-year-old male fish vendor had a 5-year history of type 2 diabetes mellitus. He visited a local hospital initially due to productive cough with fever for 1 week and body weight loss of about 6 kg within 2 months. He denied a history of traveling, having symptoms similar to co-workers or family, and contact with ill persons or animals. Chest X-ray showed left upper lung solitary opacity and chest computed tomography (CT) revealed consolidation accompanied with air bronchogram (Figure 1). Pneumonia was suspected and he was admitted

*Division of Pulmonary Medicine, Department of Internal Medicine, E-Da Hospital, I-Shou University, Kaohsiung, Taiwan; **Department of Critical Care Medicine, E-Da Hospital, I-Shou University, Kaohsiung, Taiwan
Address reprint requests to: Dr. Chien-Tung Chiu, Division of Pulmonary Medicine, Department of Internal Medicine, E-Da Hospital, I-Shou University, Kaohsiung, Taiwan, No. 1, Yida Road, Jiaosu Village, Yanchao District, Kaohsiung, Taiwan

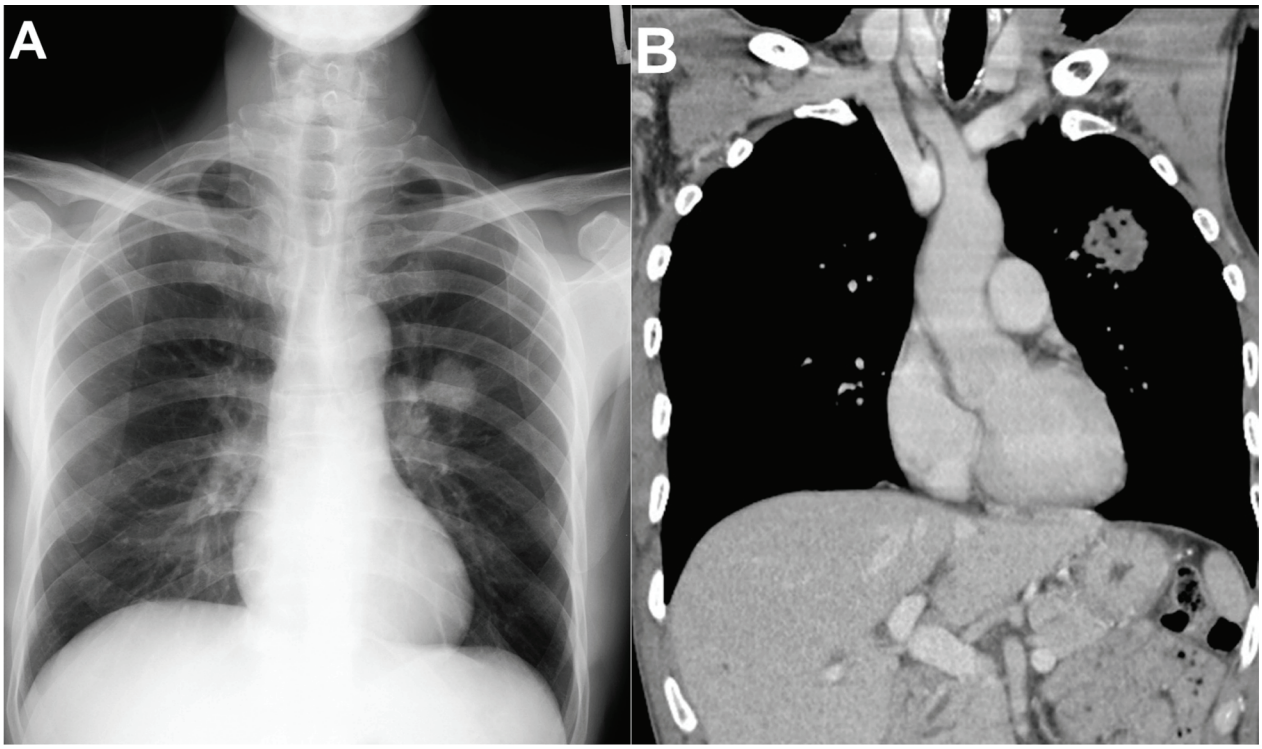

Fig. 1. A, Chest radiograph showed a left solitary lung nodule. B, Chest computed tomography showed a left upper lung nodule.

for intravenous antibiotics treatment. Follow-up chest X-ray showed no improvement after 1 month, so he was admitted to our hospital for further management.

Physical examination on hospitalization revealed no lymphadenopathy, a coarse breathing sound in the left upper lung field, regular heart beat without murmur, and no skin lesion. Chest X-ray revealed persistent left upper lung solitary ground-glass opacity. White blood-cell count was 9180/μl, with 80.6% neutrophils, 12.4% lymphocytes, and 6.6% monocytes. Carcinoembryonic antigen (CEA) was 7.12 ng/ml. Serum Cryptococcus antigen was negative. Sputum acid-fast stain, tuberculosis culture, sputum bacterial culture, and sputum fungus culture were negative. Intravenous antibiotics with amoxicillin/clavulanate were prescribed for pneumonia and CT-guided biopsy was arranged for suspected lung cancer.

The patient was discharged after antibiotics treatment for 1 week, with improved symptoms. The pathology report indicated organizing

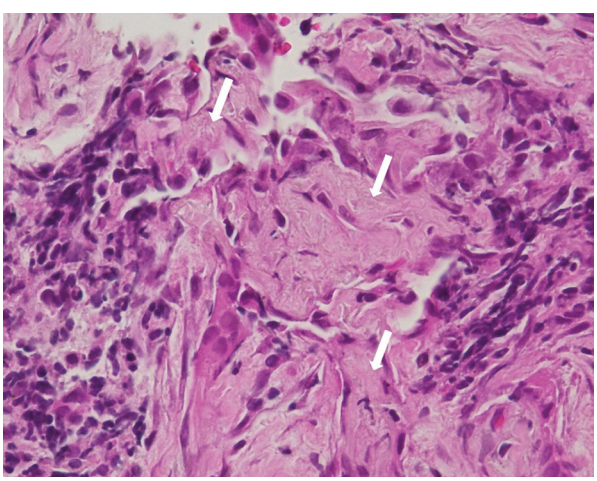

Fig. 2. Pathology showed patchy fibroblastic nodules characterized by proliferative spindle fibroblasts in a pale-staining matrix (arrow).

pneumonia (Figure 2), and the patient received oral prednisolone. However, productive cough, fever with chillness, and dyspnea developed 1 week after taking oral prednisolone, so the patient visited our emergency department. Physical examination revealed an acute ill-looking appearance with body temperature of 38.6°C, tachycardia (112 bpm), desaturation with SpO_2: 93%, and coarse breathing sounds in the bilateral lung fields. White blood-cell count was 9140/μl, with 92.4% neutrophils, 4.5% lymphocytes, and 3.0% monocytes. Platelet count was 85,000/μl; C-reactive protein was 179.8 mg/L; and influenza A and B tests were negative. Chest X-ray revealed multiple ground-glass opacities and nodular-like consolidation at the left hilar region. Empirical antibiotics with ceftriaxone were administrated. Arterial blood gas revealed respiratory alkalosis due to carbon dioxide washing out and chest X-ray revealed bilateral progressive pneumonia. The patient then was admitted to the medical intensive care unit (ICU). However, the patient's condition went downhill, so we switched antibiotics to imipenem/cilastatin, levofloxacin, and teicoplanin. Serum examinations for cryptococcal antigen, sputum acid-fast stain, tuberculosis culture, urine Legionella and pneumococcal antigen, and human immunodeficiency virus test reports were negative. Blood culture reported Gram-negative bacilli, and the antibiotics were switched to imipenem/cilastatin only.

Five days later, newly developed fever was recorded. Chest X-ray and CT revealed bilateral multiple cavitary lesions (Figure 3). Sputum and blood culture both revealed *B. pseudomallei*. We then switched antibiotics to imipenem/cilastatin plus sulfamethoxazole-trimethoprim

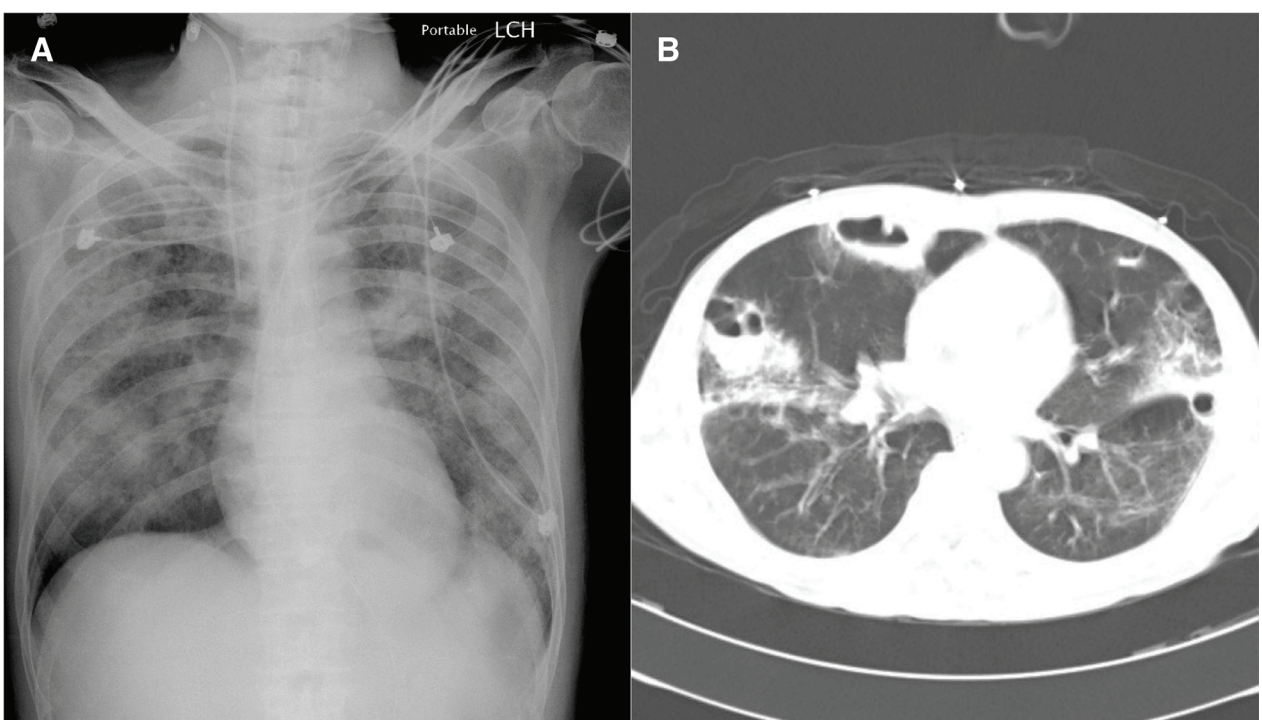

Fig. 3. A, Chest radiograph showing mixed infiltration, ground-glass patches and consolidation of the bilateral lung. B, Chest computed tomography showed bilateral multiple cavitary lesions.

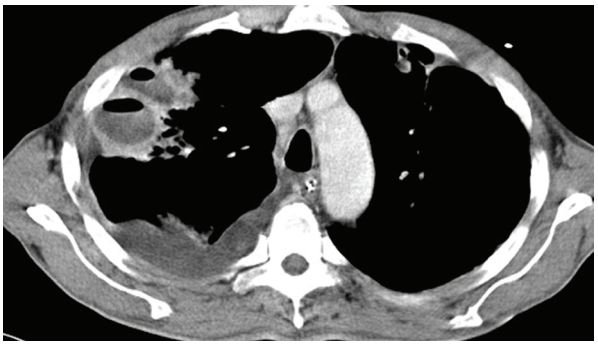

Fig. 4. Chest computed tomography showing bilateral multiple focal consolidation with variable-sized cavitary lesions and massive right pleural effusion.

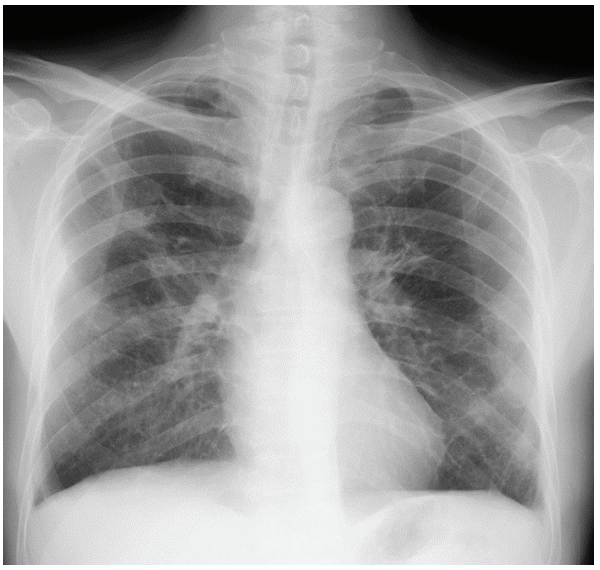

Fig. 5. Chest radiograph showing improvement in the outpatient department.

and the patient's condition improved. Follow-up chest X-ray showed improvement in the lung lesion. For further weaning from the ventilator, the patient was transferred to the respiratory care center after 20 days in the ICU. With the appearance of a skin rash, sulfamethoxazole-trimethoprim was held due to a suspected drug allergy. Fever with shock was noted after withholding sulfamethoxazole-trimethoprim for 3 days. White blood-cell count was 33,880/μl, with 89.1% neutrophils, 5.2% lymphocytes, and 5.5% monocytes. The patient was transferred back to the ICU for further care. Antibiotics were switched again to imipenem/cilastatin, sulfamethoxazole-trimethoprim, and colistin. Follow-up chest CT revealed bilateral multiple focal consolidation with variable-sized cavitary lesions and massive right pleural effusion (Figure 4). Thoracocentesis was performed with exudative pleural effusion, which grew *B. pseudomallei*.

Under treatment, the fever subsided and the patient's vital signs turned stable. The patient underwent tracheostomy due to difficulty weaning from the ventilator and was transferred to the general ward after secondary ICU admission for 2 weeks. In the general ward, antibiotics with imipenem/cilastatin plus sulfamethoxazole-trimethoprim were maintained, and then switched to meropenem plus sulfamethoxazole-trimethoprim due to dizziness. Follow-up chest X-ray showed improvement in the lung lesion. The patient was discharged with oral sulfamethoxazole-trimethoprim plus doxycycline after 5 weeks of intravenous antibiotics treatment in the ward. Follow-up chest X-ray (Figure 5) showed gradual improvement and no relapse after 6 months.

Discussion

Organizing pneumonia is defined as a process of pulmonary tissue repair that can be secondary to a lung injury, associated with another lung pathology, or cryptogenic in nature. Lung injury can be caused by infection, drug toxicity, drug intoxication, inhalation of toxic gas, aspiration of gastric contents, collagenosis, organ transplant, and radiotherapy. Lung pathology may be due to vasculitis, a tumor or pulmonary

infarct, hypersensitivity pneumonitis, eosinophilic pneumonia, and interstitial lung disease. Organizing pneumonia is considered to be cryptogenic if there is no identified etiology. Clinical characteristics include fever, cough, malaise, anorexia, and body weight loss. The diagnosis of organizing pneumonia requires a multidisciplinary approach combining clinical and radiological expertise with histopathological evidence when a lung biopsy has been performed. Corticosteroids are the current standard treatment [6-7].

Melioidosis is a tropical infectious disease caused by the Gram-negative bacilli *B. pseudomallei*. There has been an increase in reported cases in non-endemic areas because of the ease of travel, severe weather conditions, and environmental disasters. Several immunocompromised conditions, including diabetes mellitus, chronic kidney disease, hematologic disease, and cancer, have been associated with the predisposition to acquiring melioidosis. Melioidosis is intrinsically resistant to penicillin, ampicillin, secondary-generation cephalosporins, and some aminoglycosides [1,4,8-9]. Reports of pulmonary melioidosis associated with organizing pneumonia are rare. Our patient presented with solitary pulmonary opacity while receiving amoxicillin-clavulanate initially, but the condition did not improve. Pathology reported organizing pneumonia, but the clinical condition progressed into fulminant septicemia as the patient was being treated with oral steroid. For the treatment of melioidosis, ceftazidime is suggested for patients admitted to the ward and carbapenem is suggested for patients admitted to the ICU. Disease progression may be due to inadequate antibiotics treatment. Addition of sulfamethoxazole-trimethoprim is recommended for non-pulmonary melioidosis for better tissue penetration during the initial intensive therapy [1,10]. The patient was well on his way to recovery with imipenem/cilastatin plus sulfamethoxazole-trimethoprim treatment.

Post-infectious organizing pneumonia in melioidosis can easily be missed, or mistaken as lung cancer or as simple antibiotics treatment failure. Image findings of organizing pneumonia and pulmonary melioidosis may be similar. However, organizing pneumonia caused by melioidosis is rare. The duration of antibiotics treatment should be prolonged, and the proper choice of antibiotic is important. Clinicians should be aware of the possibility of melioidosis causing organizing pneumonia if there is antibiotics treatment failure, after excluding malignancy.

References

1. Wiersinga WJ, Currie BJ, Peacock SJ. Melioidosis. N Engl J Med 2012; 367(11): 1035-44.
2. Zueter A, Yean CY, Abumarzouq M, *et al*. The epidemiology and clinical spectrum of melioidosis in a teaching hospital in a North-Eastern state of Malaysia: a fifteen-year review. BMC Infect Dis 2016; 16: 333.
3. Perumal Samy R, Stiles BG, Sethi G, *et al*. Melioidosis: Clinical impact and public health threat in the tropics. PLoS Negl Trop Dis 2017; 11(5): e0004738.
4. Burivong W, Wu X, Saenkote W, *et al*. Thoracic radiologic manifestations of melioidosis. Curr Probl Diagn Radiol 2012; 41(6): 199-209.
5. Foong YC, Tan M, Bradbury RS. Melioidosis: a review. Rural Remote Health 2014; 14(4): 2763.
6. Huo Z, Feng R, Tian X, *et al*. Clinicopathological findings of focal organizing pneumonia: a retrospective study of 37 cases. Int J Clin Exp Pathol 2015; 8(1): 511-6.
7. Niksarlıoğlu EY, Özkan GZ, Bakan ND, *et al*. Cryptogenic organizing pneumonia: clinical and radiological features, treatment outcomes of 17 patients, and review of the literature. Turk J Med Sci 2016; 46(6): 1712-18.
8. Dance D. Treatment and prophylaxis of melioidosis. Int J

Antimicrob Agents 2014; 43(4): 310-8.
9. Hemarajata P, Baghdadi JD, Hoffman R, *et al*. Challenges for the clinical microbiology laboratory. J Clin Microbiol 2016; 54(12): 2866-73.
10. Zainal Abidin H, Muhd Besari A, Nadarajan C, *et al*. Acute bacteremic pneumonia due to melioidosis developing in the intensive care setting. IDCases 2017; 8: 63-5.

類鼻疽桿菌肺炎併器質化肺炎：案例報告

陳靜宜 * 魏裕峰 * 邱建通 *,**

類鼻疽（Melioidosis）為感染類鼻疽桿菌 *Burkholderia pseudomallei* 所引起的熱帶地域感染疾病，肺部是最常被影響的器官。器質化肺炎（organizing pneumonia）是肺臟針對許多不同病因所造成急性損害的一種修護反應。本文分享一個病例，初始表現為單一肺斑塊，先以抗生素 Amoxicillin-clavulanate 作為肺炎治療。單一肺斑塊病理切片報告器質化肺炎，加上口服類固醇治療後，病情惡化為敗血性休克併急性呼吸衰竭。經過加護病房照顧及抗生素 Imipenem/cilastatin 加上 Sulfamethoxazole-trimethoprim 使用，感染獲得控制，病人最後穩定出院。*(胸腔醫學 **2019; 34: 64-70**)*

關鍵詞：類鼻疽桿菌，肺類鼻疽，器質化肺炎

* 義大醫院 / 義守大學 胸腔內科，** 義大醫院 / 義守大學 重症醫學部
索取抽印本請聯絡：邱建通醫師，義大醫院 / 義守大學 胸腔內科，高雄市燕巢區角宿里義大路 1 號

Severe Hypernatremia-Induced Rhabdomyolysis with Acute Kidney Injury in an Acute Respiratory Distress Syndrome Patient – A Case Report

Shih-Min Shen, Chen-Yiu Hung, Chung-Chi Huang

Severe hypernatremia-induced rhabdomyolysis with acute kidney injury is an uncommon and potentially life-threatening clinical event. We reported the case of a 67-year-old woman with acute respiratory distress syndrome. Rhabdomyolysis with acute kidney injury was noted, and the etiology of rhabdomyolysis was hypernatremia. Because of the patient's hypernatremia, fluid overload and unstable hemodynamic status, she was placed under continuous renal replacement therapy. This report highlights an unusual cause of rhabdomyolysis in an acute respiratory distress syndrome patient and the experience of managing such a difficult clinical situation. ***(Thorac Med 2019; 34: 71-76)***

Key words: hypernatremia, rhabdomyolysis, acute kidney injury

Introduction

Severe hypernatremia is not a common condition, but is associated with a high mortality rate when values exceed 180 mEq/L. It contributes to hyperosmolality and cellular dehydration, which may lead to a variable range of neurologic manifestations, such as lethargy, weakness, irritability, seizure, and even coma [1].

Rhabdomyolysis is a potentially life-threatening syndrome. It may cause electrolyte imbalance, myoglobinuria and acute renal failure (ARF) due to muscle necrosis with intracellular constituents entering the circulation. Frequently described etiologies of rhabdomyolysis include trauma, immobilization, increased muscular activity, sepsis, exogenous toxins, underlying myopathy and muscle metabolic defects [2].

Severe hypernatremia is a condition that can induce rhabdomyolysis, but it is rarely reported. We describe the case of a patient with severe hypernatremia (171 mEq/L), rhabdomyolysis and ARF associated with hypoxic respiratory failure after an episode of influenza infection.

Case Report

A 67-year-old woman had no systemic disease before this admission. She initially had intermittent fever up to 38.2^{o} Celsius with chills. Associated symptoms included sore throat, productive cough with purulent sputum, dyspnea, mild myalgia, poor intake and diarrhea. The

Department of Thoracic Medicine, Chang Gung Memorial Hospital at Linkou, Taoyuan, Taiwan
Address reprint requests to: Dr. Chung-Chi Huang, Division of Pulmonary and Critical Care Medicine, Department of Thoracic Medicine, Chang Gung Memorial Hospital, 5 Fu-Hsing Street, Kweishan, Taoyuan 333, Taiwan

patient had no chest tightness, lethargy, or consciousness disturbance. A travel, occupation, contact and cluster (TOCC) history was also denied by the patient.

At admission, the patient's vital signs showed temperature 38.1° Celsius, pulse rate 109/min, respiratory rate 22/min, and blood pressure 122/81 mmHg; her consciousness level was E4V5M6, oriented. Physical examination revealed a symmetric breathing pattern and bilateral crackles, but no accessory muscle usage, audible heart murmur, jugular vein engorgement, or limbs edema. Initial blood hemogram and biochemical tests showed leukocytosis with a left shift (WBC 14,600/uL; segments 86%; lymphocytes 7%) and an elevated C-reactive protein (CRP) concentration (151.8 mg/L). Renal function (blood urea nitrogen 20.6 mg/dL; creatinine 0.95 mg/dL), liver function, and electrolyte level (serum sodium 137 mEq/L; serum potassium 4.7 mEq/L) were normal on the first day of ICU admission. Plain film revealed a bilateral alveolar pattern and a bilateral blunting costodiaphragmatic angle (Figure 1A).

Oseltamivir 75 mg BID and levofloxacin 750 mg QD were initially prescribed for treatment under the impression of viral pneumonia, based on the flu-like symptoms and plain film. On day 3, progressive shortness of breath with acute respiratory distress syndrome (pH 7.441, PaO_2/FiO_2 ratio 82, FiO_2 100%) caused by viral pneumonia with secondary infection was suspected. The follow-up plain film showed progressive infiltration and consolidation at the bilateral lobes (Figure 1B). Intubation and mechanical ventilation were then started. On day 6, fever subsided, but general edema was noted, and echocardiography showed pulmonary artery hypertension, dilated right atrium and ventricle, low cardiac output and bilateral systolic failure. Fluid overload with general edema was suspected. A diuretic agent, fresh frozen plasma and stored frozen plasma were prescribed for fluid control and volume expansion. Due to a gradual elevation of the serum sodium level, chemistry lab tests were performed. Serum sodium and osmolality showed 168 mEq/L and 396 mosm/KgH_2O, and urine sodium and osmolality showed 98 mEq/L and 679 mosm/KgH_2O. In order to avoid further salt input, intravenous fluid supplements of a half-saline solution, and then 5% dextrose in water were arranged. Indapamide was also prescribed for hypernatremia control, but the response was poor due to a high PaO_2/FiO_2 ratio and fluid overload. On day 23, tea-colored urine, decreased urine output (from 1,400 ml/day to 580 ml/day) and renal function (AKIN stage III [3]; blood urea nitrogen 150 mg/dL; creatinine 1.49 mg/dL) and metabolic acidosis (pH 7.182; HCO_3 19.0 mm/L; SBE -9.3 mm/L) were recorded. Biochemical tests showed serum sodium 171 mEq/L; serum potassium 5.1 mEq/L; myoglobin 93,817.8 ng/mL (RR, 14.3-65.8 ng/mL); and creatine kinase 9,980 U/L (RR, 20-180 U/L) (Table 1). Alkalization of urine with sodium bicarbonate and fluid repletion with a half-saline solution were prescribed first, but the response was limited by fluid overload and severe pulmonary edema (Figure 1C). On day 24, we arranged continuous renal replacement therapy (CRRT) because of the unstable hemodynamic status (blood pressure 64/33 mmHg) and severe hypernatremia. After 5 days of CRRT management, the patient's hypernatremia was gradually reduced from 176 mEq/L to a normal range without neurologic complication. Myoglobin, creatine kinase level and fluid status were also corrected (Table 1). However, the patient expired during the ICU course because of a new episode

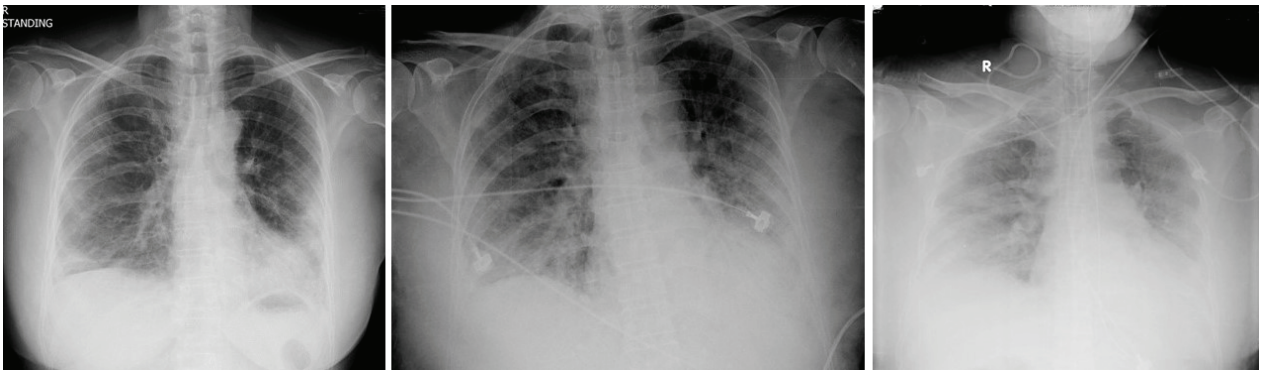

(A) (B) (C)

Fig. 1. Chest plain film showing (A) infiltration and consolidation in the bilateral lung on day 1; (B) progressive infiltration and consolidation in the bilateral lung on day 3; (C) increasing infiltration, a blunting costodiaphragmatic angle and ground glass at the bilateral lung on day 23.

of ventilator-associated pneumonia (sputum culture: multidrug-resistant *Acinetobacter baumannii*) with severe sepsis and multiple organ failure.

Discussion

Hypernatremia is a condition of total body water deficit relative to sodium content. Unreplaced water loss, water loss into cells, and sodium overload are 3 major causes of hypernatremia. Severe hypernatremia and extreme hypernatremia occur when serum sodium exceeds 160 mmol/L and 190 mmol/L, respectively. Severe hypernatremia could cause neurological symptoms, such as nausea, vomiting, muscle weakness, irritability, lethargy, confusion, seizure, myoclonic jerk and death. The management of hypernatremia includes replacement of the free water deficit, use of a diuretic agent, sodium restriction, and desmopressin if central diabetes insipidus is diagnosed [1,4]. Hypernatremia is also associated with a high risk of mortality and a poor prognosis when it occurs in critically ill patients [5]. In our case, severe hypernatremia was most likely due to sodium overload and overuse of water diuretic agents for fluid control and volume expansion. Inadequate heart functioning with activation of the renin-angiotensin-aldosterone system was also a predisposing factor.

Rhabdomyolysis is defined as muscle necrosis and leakage of intracellular muscle components into the circulation for any reason. It is usually associated with myalgia, red-brown urine and marked elevation of the serum creatine kinase level. The severity varies, and ranges from asymptomatic to life-threatening disease with the complications of electrolyte imbalances and acute kidney failure [2,6-7]. Our patient was initially diagnosed as a result of the clinically red-brown urine, and the diagnosis was confirmed by the elevated creatine kinase. Etiologies such as crush injury, overexertion, substance abuse, medications and influenza were excluded. The presence of renal failure and hypernatremia jeopardized these possible diagnoses.

Severe hypernatremia-induced rhabdomyolysis associated with acute kidney injury is rarely reported, and the mechanism is not well known. A possible hypothesis is that activation

Table 1. Laboratory Tests at Admission and During Hospitalization

Day	1	4	6	9	11	13	14	16	19	20	21	22	23	24*	25*	26*	27*	28*	29*	30*
BUN (mg/dL)	20.6	21.8	55.3	76.9	87.7	119	-	123	104	97.2	-	-	151	146	97.1	44.1	16.4	11.2	13.1	12.6
creatinine (mg/dL)	0.95	0.81	1.52	1.23	1.08	1.04	-	1.2	0.93	0.91	-	-	1.49	1.94	1.38	0.59	0.47	0.39	0.24	0.29
sodium (mEq/L)	137	135	140	147	157	162	168	171	171	172	176	171	171	162	152	141	140	139	139	138
potassium (mEq/L)	4.7	3.5	5.1	4.7	3.9	4	4.4	4.5	4.1	4.1	-	-	5.1	5.7	4.8	3.6	2.7	3.3	4.1	4.4
calcium (mg/dL)	-	-	7.4	9.3	8.7	8.8	-	8.5	-	-	-	-	7.2	7.6	7.5	8.1	8.6	8.9	8.9	8.4
myoglobin (ng/mL)	-	-	-	-	-	-	-	-	-	-	-	-	9980	11997	7705	8183	4166	2012	1084	536
CK (U/L)	-	-	-	-	-	-	-	-	-	-	-	-	93818	97367	81159	63389	36808	18824	10574	6943
CRP (mg/L)	152	131	51.4	32.7	7.92	2.52	-	2.26	2.24	-	-	-	-	-	-	-	-	-	-	-
procalcitonin (ng/mL)	-	-	-	0.49	-	0.48	-	-	-	0.22	-	-	-	-	-	-	-	-	-	6.03
urine output (ml/day)	-	-	900	2380	4150	2300	2200	2060	1600	1700	1700	1400	900	580	100	100	20	70	30	50

*: day of hemodialysis

BUN: blood urea nitrogen; CK: creatine kinase; CRP: C-reactive protein

of the muscle cells' electrogenic sodium pump was inhibited by a hyperosmolar status that damaged sodium calcium transport, which then activated protein kinases and caused muscle cell lysis. Rhabdomyolysis can change the intracellular osmoles of skeletal muscle cells, which causes a water shift from the extracellular to the intracellular, and results in progression of hypernatremia [8-9]. Conventional treatment of rhabdomyolysis is to 1) manage fluid and electrolyte abnormalities; 2) prevent acute kidney injury; 3) identify and treat the specific factors that trigger the episode. Our patient initially underwent urine alkalization and crystalloid fluid repletion, but had a poor response due to fluid overload with pulmonary edema, worsening renal function, and unstable hemodynamic status. CRRT is a reasonable option to correct fluid overload and decrease the sodium level by 10 mEq/L/day, according to current recommendations, and to avoid the risk of osmotic demyelination syndrome [1]. After management with CRRT (day 23-day 30), the patient's sodium level dropped from 176 to 138 mmol/L, and creatine kinase dropped from 93,817 to 6,943 U/L. The patient had no complication or hemodynamic change during hemodialysis.

Depending on the patient's condition, management with CRRT is a reasonable option to correct hypernatremia, rhabdomyolysis, and fluid overload with pulmonary edema when the patient has an unstable hemodynamic status. However, we need further large-scale prospective controlled studies to determine the role of other therapeutic options such as sustained low-efficiency dialysis. Influenza infection is also a cause of rhabdomyolysis, so further investigation of the relationship among influenza, hypernatremia and rhabdomyolysis may be needed.

Conclusion

Hypernatremia-induced rhabdomyolysis and acute kidney injury are an infrequent condition, but clinicians should be alert to the complication of electrolyte abnormality. Conventional management of rhabdomyolysis includes alkalization of urine, fluid repletion and intermittent hemodialysis. We have reported on our experience with CRRT in a patient with respiratory failure and hypernatremia-induced rhabdomyolysis.

Acknowledgment

We thank all staff members working in the Division of Pulmonary and Critical Care Medicine, Department of Internal Medicine, Chang Gung Memorial Hospital for their efforts.

References

1. Adrogue HJ, Madias NE. Hypernatremia. N Engl J Med 2000; 342: 1493-9.
2. Bosch X, Poch E, Grau JM. Rhabdomyolysis and acute kidney injury. N Engl J Med 2009; 361: 62-72.
3. Khwaja A. KDIGO clinical practice guidelines for acute kidney injury. Nephron Clin Pract 2012; 120: 179-84.
4. Palevsky PM, Bhagrath R, Greenberg A. Hypernatremia in hospitalized patients. Ann Intern Med 1996; 124: 197-203.
5. Lindner G, Funk GC, Schwarz C, *et al*. Hypernatremia in the critically ill is an independent risk factor for mortality. Am J Kidney Dis 2007; 50: 952-7.
6. Giannoglou GD, Chatzizisis YS, Misirli G. The syndrome of rhabdomyolysis: Pathophysiology and diagnosis. Eur J Intern Med 2007; 18: 90-100.
7. Khan FY. Rhabdomyolysis: a review of the literature. Neth J Med 2009; 67: 272-83.
8. Welt LG, Orloff J, Kydd DM, *et al*. An example of cellular hyperosmolarity. J Clin Invest 1950; 29: 935-9.
9. Yang TY, Chang JW, Tseng MH, *et al*. Extreme hypernatremia combined with rhabdomyolysis and acute renal failure. J Chin Med Assoc 2009; 72: 555-8.

嚴重高血鈉所引發的橫紋肌溶解症和併急性腎損傷在急性呼吸窘迫綜合徵病人：病例報告

沈世閔　洪禎佑　黃崇旂

嚴重高血鈉所引發的橫紋肌溶解症和併急性腎損傷為相對少見且可能存在危及生命的臨床問題。我們報告的案例為一位無特別病史的 67 歲女性，因為急性呼吸窘迫綜合徵住加護病房。住院期間，病人發生嚴重高血鈉並引起橫紋肌溶解症以及急性腎損傷的併發症。連續性腎臟替代治療用於病患體液過多、血行動力學不穩定及不正常的電解質等情況。此病例報告針對在急性呼吸窘迫綜合徵病人發現不常見原因的橫紋肌溶解症並提供處理此困難臨床狀況的經驗。*(胸腔醫學* ***2019; 34: 71-76)***

關鍵詞：高血鈉，橫紋肌溶解症，急性腎損傷

林口長庚紀念醫院　呼吸胸腔科
索取抽印本請聯絡：黃崇旂醫師，林口長庚紀念醫院　呼吸胸腔科暨重症醫學，台灣省桃園市龜山區復興街 5 號

A Neurofibromatosis Type 1 Patient with Intrathoracic Meningocele Presenting with a Huge Mass on Chest Radiography

Chin-Shui Yeh, Cheng-Hsiung Chen, Bin-Chuan Ji

An intrathoracic meningocele was diagnosed in a 37-year-old woman who had the clinical features of neurofibromatosis type 1 (NF-1), including café-au-lait spots, cutaneous neurofibromas and kyphoscoliosis. Chest radiography of this patient revealed a huge mass-like radiopaque density or consolidation in the left upper lung field. In these cases, meningocele should be differentiated from posterior mediastinal tumors such as neurofibroma, neuroblastoma, and ganglioneuroma, because NF-1 has a relatively high risk of tumor formation. Regular follow-up with periodic imaging and without surgical treatment was recommended. ***(Thorac Med 2019; 34: 77-81)***

Key words: intrathoracic meningocele, neurofibromatosis type 1

Introduction

Neurofibromatosis type 1 (NF-1) is a complex autosomal-dominant disorder caused by germline mutations in the NF-1 tumor suppressor gene. In a previous study, the gene for NF-1 was cloned on chromosome 17q11.2 [1]. Most patients with NF-1 develop café-au-lait macules, skinfold freckling, Lisch nodules and dermal neurofibromas [2]. Some individuals develop skeletal abnormalities including scoliosis, tibial pseudarthrosis and orbital dysplasia. Patients may also have brain tumors or peripheral nerve tumors including spinal neurofibromas, plexiform neurofibromas and malignant peripheral nerve sheath tumors. Learning disabilities, attention deficits, and social and behavioral problems may also be related to NF-1 [3].

A spinal meningocele is a saccular protrusion of the meninges through a dilated intervertebral foramen or a bony defect of the vertebral column [4]. NF-1 patients with kyphoscoliosis combined with intrathoracic meningocele concurrently are rarely reported [3]. In this report, we describe a female NF-1 patient presenting with a large intrathoracic mass and kyphoscoliosis that was found incidentally.

Case Report

A 37-year-old woman presented with neck pain with radiation to the left upper limbs for 2 months. No fever, chills, productive cough, exertional dyspnea or body weight loss were

Division of Chest Medicine, Department of Internal Medicine, Changhua Christian Hospital
Address reprint requests to: Dr. Chin-Shui Yeh, Division of Chest Medicine, Changhua Christian Hospital, 135 Nanxiao St, Changhua, Taiwan

noted during the most recent period. Her father had been diagnosed as having NF-1. She and 1 of her 3 sisters both developed multiple café au lait spots and dermal neurofibromas (Figure 1) on the cutaneous of the back and trunk, which were manifestations of NF-1.

The patient's chest radiography (Figure 2) revealed a 10.6 cm×8.0 cm mass-like radiopaque density or consolidation in the left upper lung field; lung cancer or pneumonia was suspected. There was an opacity in the left lower hemithorax, which was suspected to be pleural effusion. Chest CT (Figure 3) revealed a cystic lesion in the left upper lobe, originating from the spinal cord, left pleural effusion with passive atelectasis, and scoliosis of the thoracolumbar spine. The suspicious pleural effusion was obtained by sonography-guided thoracocentesis, and was found to be a very clear, colorless fluid. Laboratory data revealed RBC 200/uL, nucleated cells 3/uL, leukocytes 4/uL, neutrophils 4%, lymphocytes 79%, LDH 26 U/L, protein <1.0 g/dL, and glucose 60 mg/dL. Cytopathologic diagnosis was negative for malignant cells. The suspicious colorless pleural effusion was compatible with cerebrospinal fluid (CSF).

Magnetic resonance imaging (MRI) of the thoracic spine showed kyphosis of the upper thoracic spine with bony deformity, 2 huge meningocele formations on the left side of the lower cervical and upper thoracic spine, herniated through the C7-T1 and T3-4 intervertebral neuroforamen into the left thoracic cavity (Figure 4). Regular follow-up with periodic imaging without surgical treatment was recommended by the neurosurgeons.

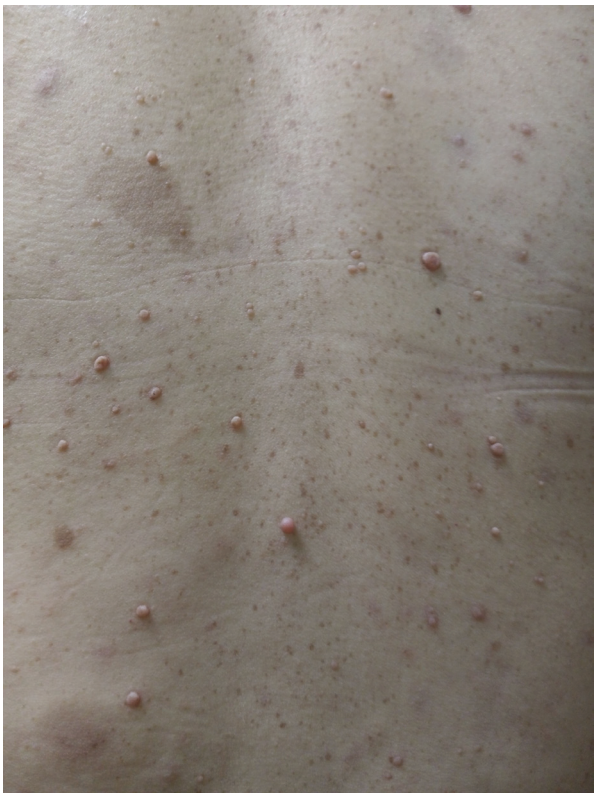

Fig. 1. Café au lait spots and dermal neurofibromas developed on the trunk skin of the patient, a characteristic of NF-1.

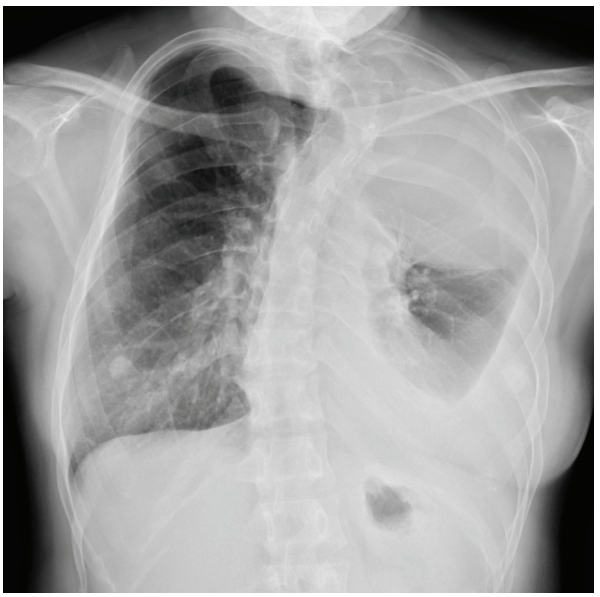

Fig. 2. Chest radiography revealed a mass-like radiopaque density or consolidation in the left upper lung field.

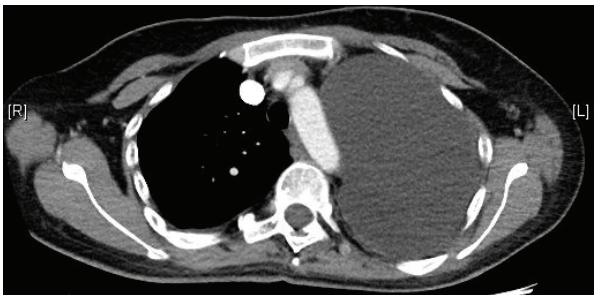

Fig. 3. Chest CT showed a cystic lesion in the left upper lobe of the lung.

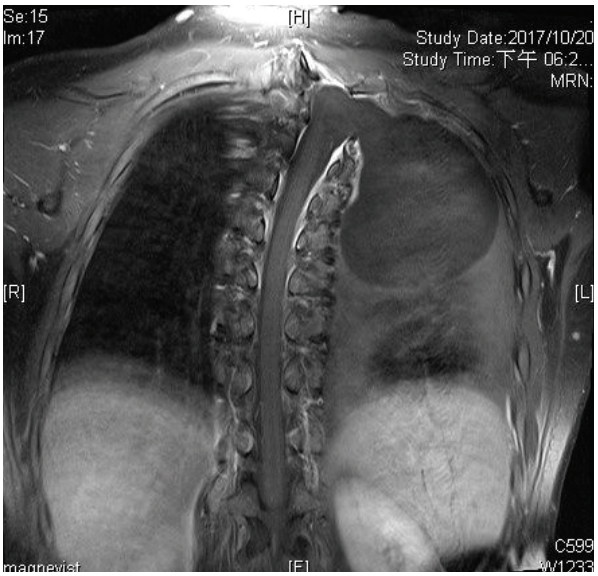

Fig. 4. Two huge meningoceles were noted on the left side of the lower cervical and upper thoracic spine in the MRI of the thoracic spine.

Discussion

A spinal meningocele is a saccular protrusion of the meninges through a dilated intervertebral foramen or a bony defect of the vertebral column. A congenital meningocele is relatively rare and usually associated with generalized mesenchymal dysplasia, such as NF-1 or Marfan syndrome [6].

A few cases of intrathoracic meningoceles associated with NF1 have been reported, although it is an uncommon pathology [7,9-10]. Case reports of concurrent NF-1, intrathoracic meningoceles and thoracic kyphoscoliosis are quite rare [8], and their pathophysiology and correlation remain unclear. Here, we reported the case of a female patient with a giant intrathoracic meningocele combined with thoracic kyphoscoliosis and NF-1.

NF-1 is a heterogeneous autosomal-dominant disease with an incidence ranging from 1 in 2,500 to 1 in 3,000 [12]. The disease commonly affects the nervous system, skin, and skeletal tissues. Scoliosis appears in 10% of NF-1 cases and is the most common skeletal manifestation of the disease [12-14]. Spinal deformity is the most common orthopedic manifestation in NF-1, and is categorized into dystrophic and non-dystrophic types [11].

Patients with an intrathoracic meningocele tend to have no symptoms, but if it is too large, it may compress a lung and neighboring organs. The symptoms and signs of intrathoracic meningocele include chest pain, a sense of pressure, chest discomfort, dyspnea at rest, and spontaneous massive hemothorax. Intrathoracic meningoceles may be either asymptomatic or result in varying degrees of respiratory dysfunction [5].

Surgery has been used to remove the meningomyelocele pouches and shunt the cyst to the subarachnoid region [10]. Surgical techniques to treat meningocele are usually undertaken only when the patient is symptomatic, and are targeted at decreasing the size of the protrusion and improving lung capacity [5]. Spontaneous hemothorax with fatal consequences may arise from bleeding of dysplastic small vessels or rupture of an aneurysm of a major intrathoracic artery. A mortality rate of up to 36% and surgical mortality of 33% have been reported as a

result of such events [15-16]. Twenty-five cases of spontaneous hemothorax have been reported in the literature [15].

We performed thoracocentesis with this patient for the purpose of reaching a differential diagnosis of the suspicious pleural effusion. Laboratory results revealed that the obtained colorless fluid was compatible with CSF. Lumbar puncture is a procedure that is often performed to obtain CSF for the diagnosis of a variety of infectious and noninfectious neurologic conditions. It is important to avoid iatrogenic infection during the CSF aspiration procedure. This patient presented no infection or neurologic symptoms or signs in the subsequent follow-up, and chest radiography revealed no increase in the size of the radiopaque density, which diminished any suspicion of a continuous CSF leak related to thoracocentesis. In our consultation, the neurosurgeon suggested regular follow-up with periodic imaging without surgical treatment, since the patient did not develop symptomatic respiratory dysfunction.

References

1. Wallace MR, Marchuk DA, Andersen LB, *et al*. Type 1 neurofibromatosis gene: identification of a large transcript disrupted in three NF1 patients. Science 1990; 249: 181-6.
2. Gutmann DH, Ferner RE, Listernick RH, *et al*. Neurofibromatosis type 1. Nat Rev Dis Primers 2017 Feb 23; 3: 17004. doi: 10.1038/nrdp.2017.4.
3. Anderson JL, Gutamann DH. Neurofibromatosis type 1. Handb Clin Neurol 2015; 132: 75-86. doi: 10.1016/B978-0-444-62702-5.00004-4.
4. Jeong JW, Park KY, Yoon SM, *et al*. A large intrathoracic meningocele in a patient with neurofibromatosis-1. Korean J Intern Med 2010 Jun; 25(2): 221-3.
5. Ebara S, Yuzawa Y, Kinoshita T, *et al*. A neurofibromatosis type 1 patient with severe kyphoscoliosis and intrathoracic meningocele. J Clin Neurosci 2003 Mar 10; 2: 268-72.
6. Oner AY, Uzun M, Tokgoz N, *et al*. Isolated true anterior thoracic meningocele. AJNR Am J Neuroradiol 2004; 25: 1828-30.
7. Das P, Goyal T, Hunt MA. Intrathoracic meningocele associated with neurofibromatosis type 1 and a novel technique for surgical repair: case report. J Neurosurg Spine 2017 Sep; 27(3): 291-4.
8. Yusuf AS, Pillai A, Menon SK, *et al*. Massive spontaneous hemothorax, giant intrathoracic meningocele, and kyphoscoliosis in neurofibromatosis type 1. J Surg Tech Case Rep 2014 Jan; 6(1): 33-6.
9. Chen HC, Chang PH, Jhang SW, *et al*. Thoracoscopic plication for a huge thoracic meningocele in a patient with neurofibromatosis. J Cardiothorac Surg 2014 May 13; 9: 85.
10. Zuo T, Ni Z, Zhou M, *et al*. Large intrathoracic meningocele in a patient with neurofibromatosis type 1. Asian Cardiovasc Thorac Ann 2014 Feb; 22(2): 219-21.
11. Cho DG, Chang YJ, Cho KD, *et al*. Collaborative treatment of huge intrathoracic meningoceles associated with neurofibromatosis type 1: a case report. J Cardiothorac Surg 2015 Nov. doi: 10.1186/s13019-015-0374-y.
12. Ferner RE. Neurofibromatosis 1 and neurofibromatosis 2: A twenty-first century perspective. Lancet Neurol 2007; 6: 340-51.
13. Tsirikos AI, Saifuddin A, Noordeen MH. Spinal deformity in neurofibromatosis type-1: Diagnosis and treatment. Eur Spine J 2005; 14: 427-39.
14. Martín-Fuentes AM, Pretell-Mazzini J, Curto de la Mano A, *et al*. High-grade spondyloretrolisthesis in a 12-year-old girl with neurofibromatosis type 1: A case report and literature review. J Pediatr Orthop B 2013; 22: 110-6.
15. Fedoruk LM, English J, Fradet GJ. Spontaneous hemothorax and neurofibromatosis: A review of a lethal combination. Asian Cardiovasc Thorac Ann 2007; 15: 342-4.
16. Conlon NP, Redmond KC, Celi LA. Spontaneous hemothorax in a patient with neurofibromatosis type 1 and undiagnosed pheochromocytoma. Ann Thorac Surg 2007; 84: 1021-3.

神經纖維瘤第一型病患合併胸腔內脊膜膨出之胸部 X 光呈現如大腫瘤

葉金水　陳正雄　紀炳銓

一位 37 歲女性被診斷出患巨大胸腔內脊膜膨出，其臨床症狀呈現出神經纖維瘤第一型之特徵包括咖啡牛奶斑、神經纖維瘤以及脊柱後側凸。病人之胸部 X 光於左上肺野呈現如腫塊般不透線的實質化病變。神經醫學專家建議此患者定期追蹤檢查暫不需外科手術治療。*(胸腔醫學 **2019; 34: 77-81**)*

關鍵詞：脊膜膨出，神經纖維瘤第一型

彰化基督教醫院　內科部　胸腔內科
索取抽印本請聯絡：葉金水醫師，彰化基督教醫院　內科部　胸腔內科，彰化市南校街 135 號

Primary Mediastinal Choriocarcinoma Complicated by Acute Respiratory Distress Syndrome and Treated with Chemotherapy Administered under Extracorporeal Membrane Oxygenation: A Case Report and Literature Review

Heng-Siang Chen, Yi-Hsin Lee*, Yao-Kuang Wu, Chih-Wei Wu

Extragonadal choriocarcinoma is a rare malignancy that occurs mostly in men, and is usually diagnosed between 20 and 30 years of age. The definite pathogenesis of extragonadal choriocarcinoma has not been clarified. Most patients have elevated serum α-fetoprotein and elevated serum β-human chorionic gonadotropin at presentation. Extragonadal choriocarcinoma is characterized by multiple metastatic lesions at the time of diagnosis; it is refractory to antineoplastic therapy, and progresses rapidly. Supportive care is a rather reasonable choice for patients with a poor performance status. Some case series have described successful chemotherapy for patients with cancer suffering from acute respiratory failure under extracorporeal membrane oxygenation (ECMO) support. Nevertheless, these reports are almost all restricted to hematologic malignancies. We present the first case of a 20-year-old man who was diagnosed with primary mediastinal choriocarcinoma and received chemotherapy under ECMO support. ***(Thorac Med 2019; 34: 82-91)***

Key words: primary mediastinal choriocarcinoma, acute respiratory distress syndrome, extracorporeal membrane oxygenation

Introduction

Choriocarcinoma is a subtype of germ cell tumors. Extragonadal germ cell tumors (EGCT) can be defined as having no evidence of a primary tumor in the testes or ovaries. EGCT represent less than 5% of all germ cell tumors [1], and usually arise in the mid-axis of the body; the most common sites are the anterior mediastinum and the retroperitoneum [2-3]. The pathogenesis of the disease has not been fully elucidated.

Primary mediastinal choriocarcinoma is a rare malignancy with an initial presentation

Department of Chest Medicine, Taipei Tzu Chi Hospital, Buddhist Tzu Chi Medical Foundation, New Taipei City, Taiwan; *Department of Pathology, Taipei Tzu Chi Hospital, Buddhist Tzu Chi Medical Foundation, New Taipei City, Taiwan

Address reprint requests to: Dr. Chih-Wei Wu, Division of Chest Medicine, Department of Internal Medicine, Taipei Tzu Chi Hospital, Buddhist Tzu Chi Medical Foundation, New Taipei City, Taiwan, No. 289, Jianguo Rd, Xindian Dist., New Taipei City 23142, Taiwan, Republic of China

of multiple pulmonary metastases, and it has a poor response to chemotherapy. Compared with their gonadal counterparts, primary mediastinal choriocarcinoma patients usually have a poor outcome, surviving no more than a few weeks. Most patients are male and are diagnosed between 20 and 30 years of age. Tumor markers typically show a marked elevation of serum β-human chorionic gonadotropin (β-HCG) and α-fetoprotein (AFP). Elevation of both markers is associated with a poor prognosis [2-3]. In the literature, thoracic images commonly present a prominent mediastinal mass with numerous bilateral pulmonary metastases [2-6]. Primary mediastinal origin is diagnosed after detailed physical and computed tomography (CT) examinations, including the thorax and abdomen. Autopsy is practically infeasible for confirmation of tumor origin.

Treatment modalities include chemotherapy, radiotherapy and surgery. The frontline therapy is chemotherapy, due to the widespread lesions at initial presentation. The chemotherapy regimen is based on its gonadal counterpart. The classic regimen is bleomycin, etoposide and cisplatin (BEP) or cisplatin, etoposide and ifosfamide (VIP) [7].

Case Report

A 20-year-old man with no past medical history visited our chest medicine outpatient department (OPD) presenting with progressive dyspnea for 1 week. The initial chest radiograph (CXR) (Figure 1A) revealed bilateral multiple variable-sized lung nodules. The chest CT scan confirmed a large anterior mediastinal mass and numerous bilateral lung nodules (Figure 2). Because of severe respiratory distress, the patient was admitted to the intensive care unit (ICU) via the emergency department on the next day.

Physical examination on admission was essentially normal. There was no gynecomastia. The testicles were equal in size and without a palpable mass. The laboratory data showed an elevated white blood cell count (WBC: 13,130/

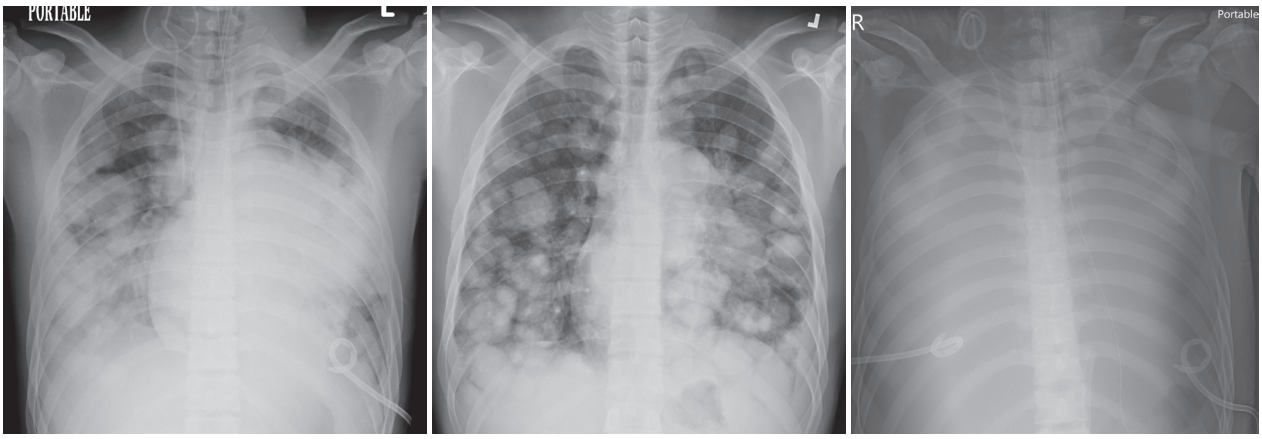

(A) (B) (C)

Fig. 1. The series of CXR changes. (A) CXR taken at the OPD on the day before ICU admission showed tumors located at the mediastinum and bilateral lungs. (B) CXR on the second hospital day revealed rapid progression of bilateral consolidation. The images included an endotracheal tube in proper position and left-side pig-tail catheter for left-side bloody effusion. (C) CXR on the ninth hospital day revealed total opacity of the bilateral lung. The images also showed the bilateral pig-tail catheter, endotracheal tube and tip of the ECMO catheter located at the inferior vena cava (IVC). Oxygen-rich blood was pumped out under ECMO through this catheter into the IVC.

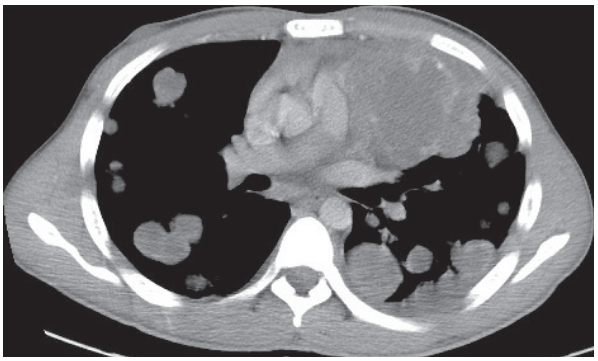

Fig. 2. Contrast-enhanced chest CT revealed a prominent anterior mediastinal tumor (size: 8x9 cm) with heterogeneous enhancement (may have been due to central necrosis or a cystic component) and bilateral metastatic tumors.

μL), elevated alanine transaminase (ALT: 87 U/L), elevated serum lactate dehydrogenase (LDH: 1,352 IU/L) and normal renal function. Considering germ cell tumors as differential diagnoses of the anterior mediastinal tumor, we checked the serum tumor markers AFP and β-HCG, and both showed marked elevation (3,824.5 ng/mL and 10,883.2 IU/L, respectively). The reference value of AFP was <20 ng/mL, and that of β-HCG was <10 IU/L. The level of serum carcinoembryonic antigen was within a normal limit.

On the first day of hospitalization, a CT-guided transthoracic needle biopsy of the mediastinal mass was performed to acquire a pathologic diagnosis. The pathologic features revealed extensive tumor necrosis with focal residual pleomorphic tumor cells. The tumor was composed of mononucleated trophoblasts and multinucleated syncytiotrophoblasts. Frequent mitosis was seen (Figure 3). Immunohistochemical staining revealed cytokeratin (+), sal-like protein4 (+), B-HCG (+), p40 (focal +), AFP (-), cluster of differentiation 30 (-), cluster of differentiation 117 (-), and thyroid transcription factor 1 (-) (Figure 4). The pathology report on the fifth day of hospitalization confirmed the diagnosis of choriocarcinoma. The final diagnosis was primary mediastinal choriocarcinoma with diffuse lung metastases.

On the second day of hospitalization, the patient received mechanical ventilator support

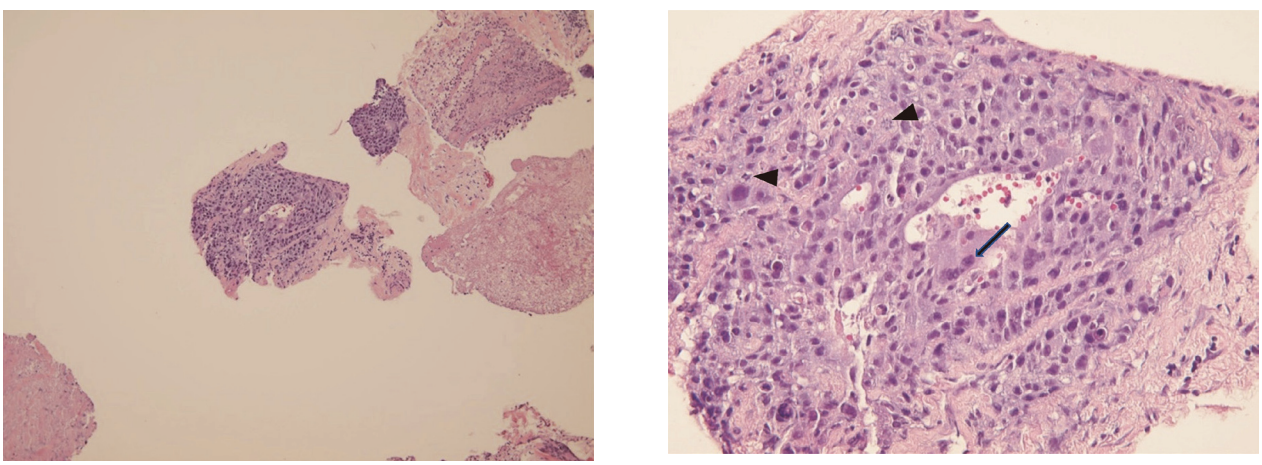

(A) (B)

Fig. 3. Histopathological features of choriocarcinoma. (A) Extensive tumor necrosis with focal residual choriocarcinoma. (B) Biphasic appearance composed of mononucleated trophoblasts and multinucleated syncytiotrophoblasts (arrow) and frequent mitoses (arrowheads). Original magnifications: (A) x100; (B) x400

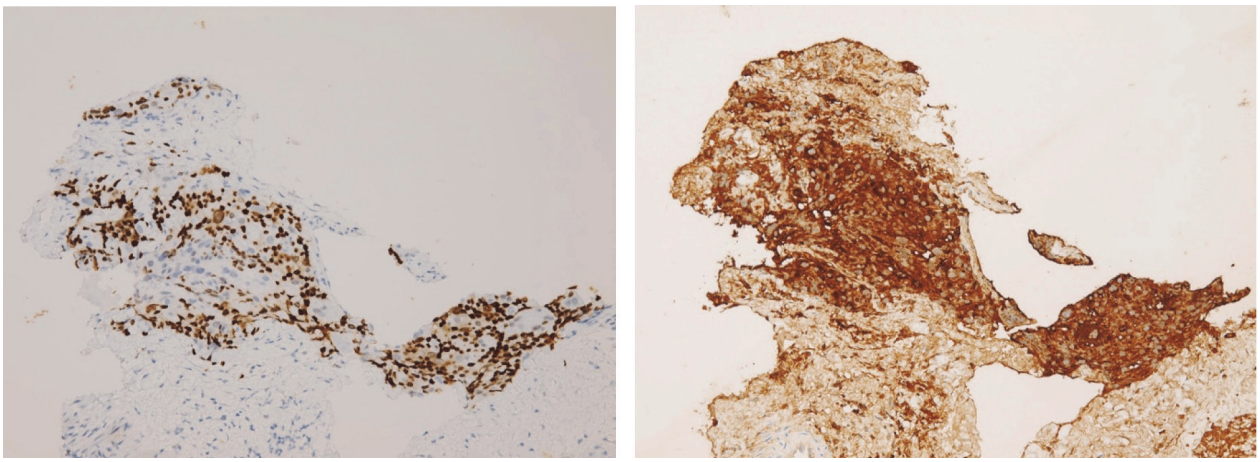

(A) (B)

Fig. 4. Immunohistochemical staining of choriocarcinoma. (A) SALL4: positive. (B) β-hCG: positive. Original magnification: 200x. [SALL4: sal-like protein 4, β-HCG: beta human chorionic gonadotropin]

due to hypoxic respiratory failure. The CXR revealed progressive consolidations at the bilateral lungs (Figure 1B). However, his oxygenation deteriorated drastically despite mechanical ventilation. On the fourth day of hospitalization, the patient received veno-venous extracorporeal membrane oxygenation (ECMO) via the femo-femoral route. We consulted the oncologist and had a detailed discussion with family members on the benefits and risks of chemotherapy administration while the patient was under this critical condition.

On the fifth day of hospitalization, chemotherapy was administered while the patient was under life support with mechanical ventilator and ECMO. The BEP regimen was cisplatin [20 mg/m^2, intravenous (IV) drip day 1-5], etoposide (25 mg/m^2, IV drip day 1-5) and bleomycin (15 unit per dose, IV drip day 1, 8, 15); cycle length=21 days; the scheduled course: 3 cycles. During chemotherapy, the patient received empiric antibiotics (i.e., linezolid, levofloxacin and imipenem) under the advice of the infectious diseases physician. The routine microbiologic cultures, including sputum, urine and blood cultures, were all negative. On the sixth day of hospitalization, acute renal failure developed, as the daily urine output was less than 300 mL. Meanwhile, the patient's blood pressure was unstable and an inotropic agent was required to maintain adequate perfusion. The nephrologist launched continuous veno-venous hemofiltration (CVVH) on the same day. Due to this episode, the day 2 (the sixth hospital day) chemotherapy regimen (cisplatin, etoposide) was held.

Under CVVH and ECMO support on the seventh and eighth day, only etoposide was given for day 3 and day 4 of chemotherapy, and cisplatin was discontinued due to renal failure. The patient's clinical status deteriorated progressively in spite of chemotherapy, antibiotics and the life support system. Hemoptysis, as well as upper gastrointestinal tract bleeding also occurred. Oliguria persisted and ECMO remained at a 100% fraction of inspired oxygen (FiO_2). The CXR at 5 AM on the ninth day revealed a dismal pulmonary condition (Figure 1C). EKG showed pulseless electrical activity

at 7 AM, and the patient expired at 8 AM on the ninth day after admission.

Discussion

We presented the case of a patient with primary mediastinal choriocarcinoma with multiple lung metastases complicated with ARDS, who received chemotherapy under mechanical ventilation, ECMO and CVVH. The main cause of ARDS may have been indirect lung injury by tumor progression. The hemoptysis exacerbated gradually during the hospital course. The tidal volume decreased progressively from 692 ml to 64 ml (Table 2). We thought the most likely causes of low tidal volume were obstruction of the large airway by the tumor and a blood clot. We did not perform diagnostic bronchoscopy because it would not have changed our treatment plan.

We reviewed the literature on primary mediastinal choriocarcinoma -- almost all reported cases had similar clinical features, and there were many similarities between our case and cases in the literature. In a series of 8 cases of primary mediastinal choriocarcinoma in 1997 [2], all patients were men between the ages of 21 and 63 years (mean, 42 years). Clinical symptoms included shortness of breath, chest pain, cough, and superior vena cava syndrome; 1 patient also had gynecomastia. All patients presented with large anterior mediastinal masses on CXR that measured an average of 10 cm at the greatest diameter. Immunohistochemistry revealed the tumors were notable for strong β-HCG positivity. Seven patients presented at the time of diagnosis with thoracic and extrathoracic (liver, adrenal, kidney, and spleen) metastases. The tumor in 1 case was entirely confined to the mediastinum. All patients died over a period of 1 to 2 months.

We searched the literature for the latest case reports. Zhang reported a 20-year-old male who suffered dyspnea and hemoptysis for 2 weeks [4]. The contrast chest CT showed a huge mediastinal tumor with bilateral pulmonary metastatic tumors. The tumor marker also showed elevated β-HCG (>500,000 IU/L) and AFP (104.9 ng/mL). The patient received an EMA-VO chemotherapy regimen, including etoposide, methotrexate, actinomycin D, cyclophosphamide, and vincristine/oncovine, but suffered a catastrophic outcome, similar to our patient. During chemotherapy, the patient deteriorated with progressively decreasing pulse oxygen saturation (60%~30%), significant respiratory distress and massive hemoptysis. But, the patient was not placed under invasive mechanical ventilator support. The patient was discharged voluntarily and died after 70 days of symptoms presentation. In another case from China [6], a 26-year-old male patient visited the hospital due to hemoptysis for 2 weeks. The chest CT image also showed mediastinal tumor with bilateral pulmonary metastasis. The tumor marker showed elevated β-HCG. The patient was placed on an EMA-VO chemotherapy regimen, but the paper was published during the chemotherapy course, so the survival result was unavailable. In Canada, a 25-year-old man with a past history of Hodgkin lymphoma presented with a persistent cough, hemoptysis, and right supraclavicular lymphadenopathy [8]. His clinical condition deteriorated rapidly, so he was given chemotherapy with invasive mechanical ventilator support. Despite aggressive treatment, the patient died within 2 weeks. In Japan, A 30-year-old man presented with cough and bloody sputum [9]. The chest CT revealed a large mediastinal mass and multiple nodular

Table 1. Serial PaO_2/FiO_2

Hospital day	1	2	3	4	5	6	7	8	9
PaO_2/FiO_2	unavailable	135	117	84	139	298	81	60	60
Comment	Not intubated	30 minutes after mechanical ventilation begun	nil	1 hour before ECMO launch	Chemo-therapy day 1	CVVH day 1 & inotropic agents day 1	nil	nil	expired

Table 2. Serial Tidal Volume

Hospital day	1	2	3	4	5	6	7	8	9
Ventilator tidal volume (ml)	Not intubated, under non-rebreathing mask	692	633	643	461	411	239	70	64
Special events	CT-guided lung biopsy	Mechanical ventilator day 1	nil	ECMO day 1	Chemo-therapy day 1	CVVH day 1 & inotropic agents day 1	nil	nil	expired

Table 3. Serial Urine Output and Serum Renal Function Data (BUN denotes serum blood urea nitrogen; Cr denotes serum creatinine)

Hospital day	1	2	3	4	5	6	7	8	9
Daily urine output (ml)	2640	1230	750	900	750	280	155	376	No record
BUN (mg/dL)	No test	6	No test	No test	17	19	31	33	35
Cr (mg/dL)	0.9	0.8	No test	No test	0.6	0.9	1.7	1.8	1.7
Special events	CT-guided lung biopsy	Mechanical ventilator day 1	nil	ECMO day 1	Chemo-therapy day 1	CVVH day 1 & inotropic agents day 1	nil	nil	expired

shadows in both lungs. The serum β-HCG level was remarkably elevated. He was given a VIP chemotherapy regimen, and the tumor size regressed initially. However, there was a rapid relapse, and the patient died 7 months after his first hospital visit. In Taiwan, Hsiao reported the case of a patient with primary mediastinal choriocarcinoma [10]. The patient had a mediastinal tumor with bilateral lung metastasis and elevated serum β-HCG. There was no obvious response to cisplatin-based chemotherapy and the patient died as a result of respiratory failure, which may have been due to the extended multiple pulmonary metastases.

Our patient suffered from hypoxic respiratory failure and was placed on invasive mechanical ventilator support on the second hospital day. Thirty minutes after launching the invasive mechanical ventilator with a 90% FiO_2, we checked the arterial blood gas (ABG) and the result showed oxygen partial pressure (PaO_2) of 108 mmHg. The PaO_2/FiO_2 ratio was 120. We used a lung protective strategy, including low tidal volume and high positive end expiratory pressure (PEEP). The patient was 178 cm in height, so the predicted body weight (PBW) was 73 kg. The target tidal volume of our lung protective strategy was 8 ml/kg PBW (Table 2). The CXR and ABG worsened progressively after mechanical ventilation was begun. Before ECMO launch, the ventilator setting was a pressure-assisted control mode: PEEP=12 mmHg, inspiratory pressure=14 cmH_2O, the upper limit of peak inspiratory pressure=30 cmH_2O, and the minimal backup of respiratory rate=12/minutes. On the fourth hospital day, ABG showed PaO_2=76 mmHg and FiO_2=90%, and the PaO_2/FiO_2 ratio=84. Based on this ABG data, ECMO was launched. Under ECMO support, the PaO_2/FiO_2 ratio improved for only 2 days. With disease progression, the PaO_2/FiO_2 worsened again (Table 1). After beginning ECMO, the CXR, hemodynamic status and PaO_2/FiO_2 continued to worsen. We did not arrange another chest CT scan, because the examination would have put the patient, who was already in a grave condition, at risk and it would not have changed our management.

As for the chemotherapy regimen of BEP and VIP, bleomycin is well known for its pulmonary toxicity and ifosfamide for severe myelosuppression. Since pulmonary infection and sepsis were ongoing and immunity was the primary concern, we chose a BEP regimen for this patient. The hemoptysis and progressive lung consolidation may have been related to tumor progression or heparin use for ECMO. The independent risk factors for bleomycin-induced pneumonitis are renal function, cumulative dose of bleomycin (>300 U), age (>40 years old) and advanced stage of the primary disease. The median time from the initiation of bleomycin administration to the manifestation of lung toxicity was 4.2 months (range 1.2-8.2) [11]. Because of the low bleomycin dose (15 U) and short interval (2 days) between chemotherapy and lung injury, bleomycin-induced lung toxicity was less likely. On the other hand, surgery is generally reserved for emergencies such as large airway compression or hemothorax. Radiotherapy is generally ineffective.

Acute renal failure occurred on the sixth day of hospitalization (Table 3). The most likely cause of acute renal failure was pneumonia and septic shock. This scenario is frequently repeated in the ICU. Other possible causes included the non-steroidal anti-inflammatory drug (naproxen) used for fever control and chemotherapy (cisplatin).

Supportive care is an alternative choice for cancer patients with a poor performance status. Some malignant diseases that affect young patients have a rapidly progressive nature. Aggressive treatment in a situation with organ failure could be provided after thorough discussion with the patient and family. In this case, the patient's condition rapidly deteriorated to ARDS requiring ECMO. To the best of our knowledge, there are few adult case reports describing chemotherapy delivered under ECMO. The ma-jority of underlying diseases is hematologic malignancy, although there was a patient with gestational choriocarcinoma [12-14]. In a case series [12], 14 patients with hema-tologic

malignancy received ECMO support because of acute respiratory failure; 5 pa-tients received chemotherapy under ECMO support, and 4 were discharged alive from the hospital. Allain presented a case of primary cardiac lymphoma [13], in which a 65-year-old immunocompetent male patient suffered from cardiogenic shock requiring emergency ECMO. Chemotherapy was delivered under ECMO support, and the pa-tient was progressively weaned from mechanical support. Six months later, he had fully recovered. A 22-year-old female patient with gestational choriocarcinoma suffered from massive tumor pulmonary embolism and received venoarterial ECMO because of hemodynamic instability [14]. The patient was treated with chemotherapy in the pres-ence of ECMO and responded well. She was discharged after 3 months.

Whether to use supportive care or aggressive chemotherapy delivered under ECMO is a dilemma. Since our patient was young and in a dire condition, we did not give up and chose aggressive treatment. Unfortunately, the efforts did not pay off in the end.

Conclusion

In a patient with primary mediastinal choriocarcinoma, early diagnosis is essential for early treatment and a better outcome. Its rapidly progressive nature, however, may result in respiratory failure and organ dysfunctions that require mechanical ventilation and life support such as ECMO and CVVH. The efficacy of chemotherapy under these conditions is not well established. Here, we presented the first case of mediastinal choriocarcinoma in which the patient received chemotherapy under CVVH and ECMO. Although the outcome in this case was fatal, whether to use supportive care or aggressive treatment with patients in this critical condition needs further study.

References

1. Collins DH, Pugh RC. Classification and frequency of testicular tumors. Brit J Urol 1964; 36 (Supplement): 1-11.
2. Moran CA, Suster S. Primary mediastinal choriocarcinomas: a clinicopathologic and immunohistochemical study of eight cases. Am J Surg Pathol 1997 Sep; 21(9): 1007-12.
3. Bokemeyer C, Nichols CR, Droz JP, *et al*. Extragonadal germ cell tumors of the mediastinum and retroperitoneum: results from an international analysis. J Clin Oncol 2002 Apr 1; 20(7): 1864-73.
4. Zhang S, Gao H, Wang XA, *et al*. Primary choriocarcinoma in mediastinum with multiple lung metastases in a male patient: A case report and a review of the literature. Thorac Canc 2014 Sep; 5(5): 463-7.
5. Zhang J, Wang ZJ, Y B, *et al*. Biochemical remission by chemoradiotherapy in male mediastinal choriocarcinoma with diffuse lung metastasis: A case report. Oncol Letters 2016 Apr; 11(4): 2615-8.
6. Luo M, Peng H, Song M, *et al*. Primary mediastinal choriocarcinoma: A case re-port and literature review. Zhong Nan Da Xue Xue Bao Yi Xue Ban 2017 Oct 28; 42(10): 1222-7.
7. Hinton S1, Catalano PJ, Einhorn LH, *et al*. Cisplatin, etoposide and either bleo-mycin or ifosfamide in the treatment of disseminated germ cell tumors: final analysis of an intergroup trial. Cancer 2003 Apr 15; 97(8): 1869-75.
8. Lam S, Rizkalla K, Hsia CC. Mediastinal choriocarcinoma masquerading as relapsed Hodgkin lymphoma. Case Reports in Oncol 2011 Sep-Dec; 4(3): 512-6.
9. Yamane T1, Egawa H, Deguchi N, *et al*. A case of pri-mary mediastinal choriocarcinoma. Nihon Kokyuki Gakkai Zasshi 2006 Jan; 44(1): 48-54.
10. Hsiao HH, Liu YC, Tsai HJ, *et al*. Poor outcomes in patients with primary malignant mediastinal germ-cell tumors. Kaohsiung J Med Scien 2005 Dec; 21(12): 561-5.

11. O'Sullivan JM, Huddart RA, Norman AR, *et al*. Predicting the risk of bleomycin lung toxicity in patients with germ-cell tumours. Ann Oncol 2003 Jan; 14(1): 91-6.
12. Wohlfarth P, Ullrich R, Staudinger T, *et al*. Extracorporeal membrane oxygena-tion in adult patients with hematologic malignancies and severe acute respiratory fail-ure. Crit Care 2014 Jan 20; 18(1): R20.
13. Allain G, Hajj-Chahine J, Lacroix C, *et al*. Primary cardiac lymphoma complicat-ed by cardiogenic shock: successful treatment with chemotherapy delivered under ex-tracorporeal membrane oxygenation support. Eur J Cardio-Thorac Surg 2015 Dec; 48(6): 968-70.
14. Chung JH, Yeo HJ, Cho HM, *et al*. Treatment of pulmonary tumor embolism from choriocarcinoma: extracorporeal membrane oxygenation as a bridge through chemotherapy. Cancer Res Treat 2017 Jan; 49(1): 279-82.

原發性縱隔腔絨毛膜癌併發急性呼吸道窘迫症候群，在葉克膜氧合器支持下接受化學治療：個案報告與文獻回顧

陳亨翔　李懌鑫 *　吳耀光　吳智偉

性腺外絨毛膜癌是一種罕見的惡性腫瘤，大部分個案為男性。它的確切致病機轉目前仍不清楚。它的好發年齡為 20 至 30 歲的年輕男性。大部分的病患在罹病初期，血清中的甲型胎兒蛋白及乙型絨毛膜促性腺激素會顯著升高。它的病程進展迅速，在初診斷時常合併多處轉移，且對化學治療反應不佳。支持性治療對於體力不佳的病患來說是一個合理的選擇。文獻上，在併發急性呼吸窘迫症候群且需葉克膜氧合器支持的癌症病患，此時注射化學治療，有少數成功的個案報告。然而，幾乎這類型的個案皆為血液惡性腫瘤的患者。我們報告一位原發性縱隔腔絨毛膜癌的 20 歲男性年輕病患，在併發急性呼吸窘迫症候群且接受葉克膜氧合器支持的狀況下，文獻上第一位接受化學治療的個案。*(胸腔醫學 **2019; 34: 82-91**)*

關鍵詞：原發性縱隔腔絨毛膜癌，急性呼吸窘迫症候群，葉克膜氧合器

台北慈濟醫院　內科部　胸腔內科，* 台北慈濟醫院　病理科
索取抽印本請聯絡：吳智偉醫師，台北慈濟醫院　內科部　胸腔內科，23142 新北市新店區建國路 289 號